國立臺灣大學醫學院暨工學院醫學工程學研究所

博士論文

Institute of Biomedical Engineering

College of Medicine and College of Engineering

National Taiwan University

Doctoral Dissertation

溫感性甲殼素/明膠/甘油磷酸水膠做為阿魏酸持續釋放於髓核再生之應用

Thermosensitive Chitosan/Gelatin/Glycerol Phosphate Hydrogel as a Sustained Release System of Ferulic Acid for Nucleus Pulposus Regeneration

鄭詠馨

Yung-Hsin Cheng

指導教授：林峯輝 博士

Advisor: Feng-Huei Lin, Ph.D.

中華民國 101 年 6 月

June, 2012

中文摘要

椎間盤退化與椎間盤突出及背痛有高度的相關性，這些病徵增加了健康照護的支出。椎間盤退化過程可分為五個階段，在退化的第一至二階段時，並沒有明顯的病徵出現，但可透過核磁共振或電腦斷層掃描檢查來追蹤，臨床上一般並不會在此階段給予治療。近來的文獻指出，活性氧自由基不僅會加速椎間盤退化的過程，且會造成髓核細胞的凋亡和細胞外基質的降解。阿魏酸是一種抗氧化物並且可以較穩定地存在於空氣中；阿魏酸被證實對於活性氧自由基所引起的相關疾病具有預防的效果。本研究的目的除了評估阿魏酸對於雙氧水所引起的氧化壓力導致髓核細胞傷害的可能治療效果外，並評估利用溫感性甲殼素/明膠/甘油磷酸水膠做為阿魏酸持續釋放早期治療椎間盤退化的可行性。

在本研究中的試驗結果指出，500 μM 為阿魏酸對紐西蘭兔的髓核細胞的安全閥值，利用阿魏酸治療被雙氧水所引起的氧化壓力所傷害的髓核細胞，其 *aggrecan*, *type II collagen* 和 *BMP-7* 的基因表現可以有顯著的提升，而 *MMP-3* 的表現量有顯著的下降，而硫酸化葡萄胺聚醣含量有顯著的上升，細胞凋亡的情形也有顯著的抑制。而以甲殼素/明膠/甘油磷酸水膠做為阿魏酸持續釋放的試驗中，阿魏酸可以從水膠中緩釋，包覆阿魏酸的水膠除了能提升被雙氧水所引起的氧化壓力所傷害的髓核細胞中 *aggrecan* 和 *type II collagen* 基因的表現量外，並能抑制 *MMP-3* 的表現量，而在硫酸化葡萄胺聚醣生成量及 alcian blue 的染色的結果指出，包覆阿魏酸的水膠可以使受傷害的髓核細胞恢復到正常髓核細胞的表現量，另外在 caspase-3 和 TUNEL 的染色結果上，也指出其細胞凋亡的情形可以被顯著抑制。在本研究中證明，阿魏酸可成功藉由 N-(3-dimethylaminopropyl)-N'-ethylcarbodiimide (EDC)/ N-hydroxysuccinimide (NHS)固定於甲殼素/明膠/甘油磷酸水膠上；在中性環境下，該水膠之成膠溫度為 31.8°C，而以阿魏酸固定於甲殼素/明膠/甘油磷酸上的水膠治

療被雙氧水所引起的氧化壓力所傷害的髓核細胞，可顯著的提升受傷害細胞中 *aggrecan* 和 *type II collage* 的表現量，並抑制其 *MMP-3* 的表現量；此外，硫酸化葡萄胺聚醣生成量也能恢復到正常的水平，另外在 caspase-3 和 TUNEL 的染色結果中顯示，細胞凋亡的情形可以被有效的抑制。

綜合上述，本研究的試驗結果指出阿魏酸可做為髓核再生的治療分子，而溫感性甲殼素/明膠/甘油磷酸水膠可做為阿魏酸長期釋放的良好載體，將阿魏酸固定於甲殼素/明膠/甘油磷酸水膠上可有效延長釋放的時間；結合阿魏酸及溫感性甲殼素/明膠/甘油磷酸水膠顯然可以有效治療因氧化壓力所傷害的髓核細胞，在未來更可應用於髓核再生的微創手術中。

關鍵字: 髓核、阿魏酸、氧化壓力、溫感性水膠、抗氧化劑

ABSTRACT

Disc degeneration is strongly associated with back pain and herniation that increase the costs of health care. The degeneration of intervertebral disc (IVD) could be divided into 5 stages. In the first and second stages, there are no significant symptoms but could be traced by magnetic resonance imaging or computed tomography-scan. Generally, no aggressive treatment would be processed in the clinics. Recent studies indicated that overproduction of reactive oxygen species (ROS) may accelerate the degenerative process of IVD and associate with apoptosis of nucleus pulposus (NP) cells and degradation of extracellular matrix. Ferulic acid (FA) is an excellent antioxidant and relatively stable in air. FA has been proven to have ability to prevent ROS-induced diseases. The object of the study was aimed to evaluate the possible therapeutic effect of FA on hydrogen peroxide (H_2O_2)-induced oxidative stress NP cells and the feasibility of use the thermosensitive chitosan/gelatin/glycerophosphate (C/G/GP) hydrogel as a sustained release system of FA for early treatment in IVD degeneration.

In the study, NP cells were harvested from the IVD of New Zealand rabbits. The results showed that 500 μM of FA might be the threshold to treat NP cells without cytotoxicity. Post-treatment of FA on H_2O_2-induced oxidative stress NP cells significantly up regulated the expression of *aggrecan*, *type II collagen* and *BMP-7* and

down regulated the expression of *MMP-3* in mRNA level. Post-treatment of FA on H_2O_2-induced oxidative stress NP cells could restore the production of sulfated glycosaminoglycans (GAGs) and inhibit the apoptosis caused by H_2O_2. The results showed that the release of FA from C/G/GP hydrogel could decrease the H_2O_2-induced oxidative stress. Post-treatment of FA-incorporated C/G/GP hydrogel on H_2O_2-induced oxidative stress NP cells showed up-regulation of *aggrecan* and *type II collagen* and down-regulation of *MMP-3* in mRNA level. The results of sulfated GAGs to DNA ratio and alcian blue staining revealed that the GAGs production of H_2O_2-induced oxidative stress NP cells could reach to normal level. The results of caspase-3 activity and TUNEL staining indicated that FA-incorporated C/G/GP hydrogel decreased the apoptosis of H_2O_2-induced oxidative stress NP cells. The results showed that FA was successfully immobilized on C/G/GP hydrogel by N-(3-dimethylaminopropyl)-N'-ethylcarbodiimide (EDC) and N-hydroxysuccinimide (NHS) crosslinking method. The gelation temperature of the FA-immobilized C/G/GP hydrogel was 31.80 °C under neutral pH. Post-treatment of FA-immobilized C/G/GP hydrogel on H_2O_2-induced oxidative stress NP cells showed down-regulation of *MMP-3* and up-regulation *aggrecan* and *type II collagen* in mRNA level. The sulfated GAGs production of H_2O_2-induced oxidative stress NP cells could be increased to the normal level in the post-treatment of FA-immobilized C/G/GP hydrogel group. The results of

caspase-3 activity and TUNEL staining showed that the apoptosis of H_2O_2-induced oxidative stress NP cells could be inhibited by post-treatment of FA-immobilized C/G/GP hydrogel.

From the results of the study, FA could be used as a therapeutic molecule for NP regeneration and FA-incorporated C/G/GP hydrogel might be potentially applied as a long-term release system. The immobilization of FA on C/G/GP hydrogel could significantly prolong the release period of FA. These results suggest that combination of FA and thermosensitive C/G/GP hydrogel can treat NP cells from the damage caused by oxidative stress and may apply in minimally invasive surgery for NP regeneration in the future.

Keyword: nucleus pulposus; ferulic acid; oxidative stress; thermosensitive hydrogel; antioxidant

TABLE OF CONTENTS

LIST OF CHARTS

CHAPTER 1

CHAPTER 2

CHAPTER 4

LIST OF TABLES

CHAPTER 1

CHAPTER 2

LIST OF ABBREVIATIONS

AF	Annulus Fibrosus
BMP	Bone Morphogenic Protein
CEP	Cartilage Endplate
CL	Chemiluminescence
C/G/GP	Chitosan/Gelatin/β-glycerophosphate
C/GP	Chitosan/β-glycerophosphate
cDNA	Complementary DNA
c-Apaf-1	Cytochrome Apoptotic Protease Activating Factor-1
DISC	Death-inducing Signaling Complex
DNA	Deoxyribonucleic Acid
DMMB	Dimethylmethylene Blue
DMSO	Dimethyl Sulfoxide
DMEM-F12	Dulbecco's Modified Eagle's Medium-nutrient Mixture F-12 Ham Medium
EDC	*N*-(3-dimethylaminopropyl)-*N′*-ethylcarbodiimide
ECM	Extracellular Matrix
ELISA	Enzyme-linked Immunosorbent Assay
FADD	Fas-associated Protein with Death Domain
FA	Ferulic Acid
β-GP	Glycerol 2-phosphate Disodium Salt Hydrate
GAG	Glycosaminoglycan
HSF	Heat-shock Transcription Factor
H_2O_2	Hydrogen Peroxide
iNOS	Inducible Nitric Oxide Synthase
IGF	Insulin-like Growth Factor
IL	Interleukin
IVD	Intervertebral Disc
LDH	Lactate Dehydrogenase
MMP	Matrix Metalloproteinase
MAP	Mitogen-activated Protein
NF-κB	nuclear factor-kappa B
NHS	*N*-hydroxysuccinimide
NO	Nitric Oxide
NP	Nucleus Pulposus
OD	Optical Density

PBS	Phosphate Buffered Saline
ROS	Reactive Oxygen Species
pRB	Retinoblastoma Protein
RT-PCR	Reverse Transcription Polymerase Chain Reaction
RNA	Ribonucleic Acid
TNBS	2, 4, 6-trinitrobenzenesulfonic Acid Solution
TUNEL	Terminal Deoxynucleotidyl Transferase dUTP Nick End Labeling
TIMP	Tissue Inhibitors of Metalloproteinase
TGF	Transforming Growth Factor
TNF	Tumor Necrosis Factor
t-Bid	Truncated-Bid
UV	Ultraviolet
UV-VIS-NIR	Ultraviolet-Visible-Near Infrared
VB	Vertebral Body
WST	Water Soluble Tetrazolium Salt

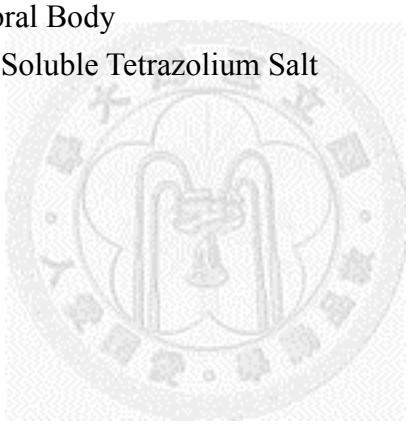

CHAPTER 1 INTRODUCTION

1.1 Structure and function of intervertebral disc

Intervertebral disc (IVD) lies between vertebral bodies (VBs) and consists of central nucleus pulposus (NP), outer annulus fibrosus (AF), and upper and lower cartilage endplates (CEPs) (Fig. 1). The main components of IVD are water, proteoglycans and collagen, which provide adequate mechanical strength to resist the external stress. Collagen network provides the tensile strength to the IVD and anchors the tissue to the bone; proteoglycans attract and retain water in the IVD that serve to resist compressive loads [1].

The IVD possesses a variety of collagen in the extracellular matrix (ECM). Type I and II collagen (approximately 80%) are the most abundant collagen in the disc matrix. The AF consists mostly of Type I collagen with small amounts of Type III, V (3%), VI (10%) and IX (1%-2%) collagens. The NP consists mainly of Type II collagen and only small amounts of Type VI (15%-20%), IX (1%-2%), XI (3%) collagens [2-3].

The IVD contains a variety of proteoglycans, including aggrecan, versican, hyaluronan, decorin, biglycan and lumican. Proteoglycan is constructed of glycosaminoglycans (GAGs) which are attached to the protein core of aggrecan.

Aggrecan is the most abundant component of the proteoglycans in the disc matrix and possesses chondroitin sulfate and keratan sulfate. Proteoglycans are interacted to hyaluronic acid to form the large aggregates. [2-3]

The NP is a gelatinous structure and composed mainly of type II collagen and proteoglycans which are organized randomly. NP contains the chondrocyte-like cell and the cell density of NP is approximately 4 x 10^6 per cm^3. AF is a lamellae structure which composed mainly of type I collagen and elastin fibers. AF contains fibroblast-like cell and the cell density of AF is about 9 x 10^6 per cm^3. In the normal disc, the percentage of type I and type II collagen is about 70% and 20% of the dry weight in the AF and NP, respectively. The proteoglycans and water content are both higher in the NP (approximately 50% and 80% of wet weight, respectively) than in the AF (around 20% and 70% of wet weight, respectively) [1-3]. The CEP is a hyaline cartilage which is an interface between the VB and IVD. The IVD is avascular, the exchange of nutrients and metabolic waste products of disc is diffused mainly through the CEP. Although small blood vessels can be found in the outer AF, they do not penetrate into inner AF and NP. The CEP serves as a selectively permeable barrier to nutrients and solutes. Small molecules such as water, oxygen and amino acids can directly penetrate the CEP by diffusion, but anions and large molecules are partially excluded. The

diffusion gradient of oxygen, glucose and lactate from upper to lower CEP has been observed in the recent years (Fig. 2). The center of the disc is at low glucose and oxygen and lactic acid concentration is highest in the center of the disc. The normal range for the pH of the disc is 6.9 to 7.2 [3-4].

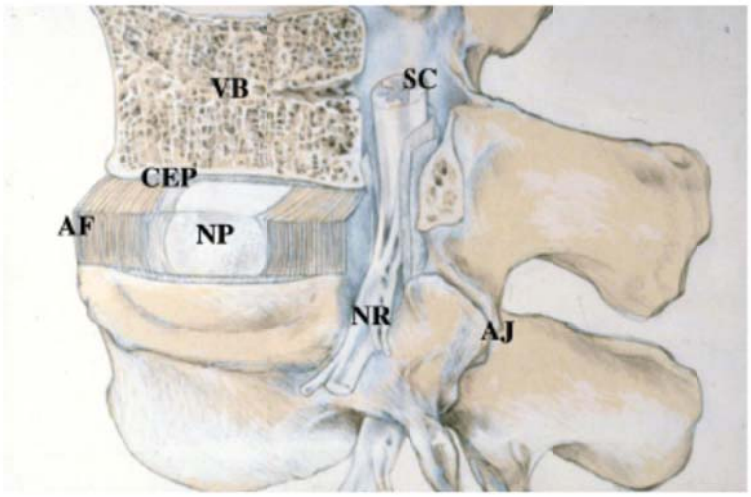

Fig. 1. 1 A schematic diagram of a spinal segment and the intervertebral disc [1].

Nucleus pulposus (NP); annulus fibrosus (AF); cartilage endplate (CEP); vertebral body (VB); spinal cord (SC); nerve root (NR); apophyseal joints (AJ)

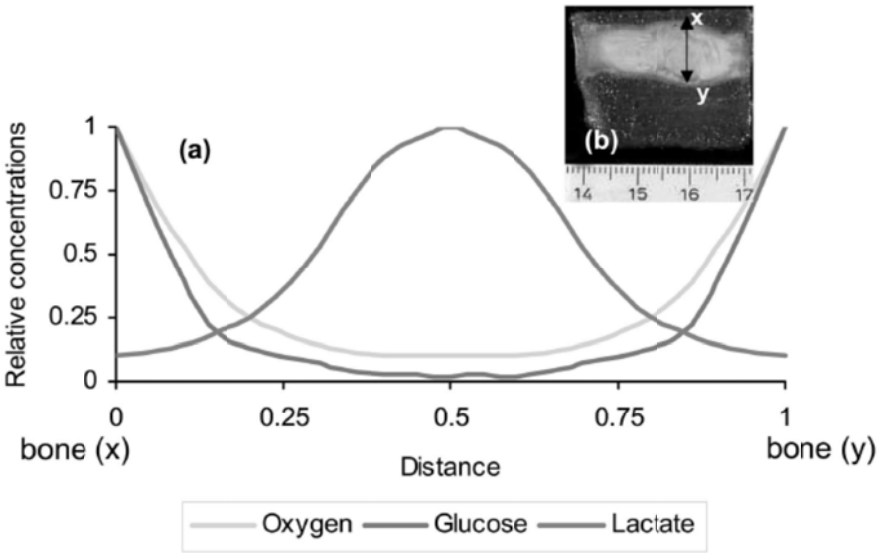

Fig. 1. 2 Schematic view of nutrient gradients across the disc [4]

1.2 Intervertebral disc degeneration

The IVD degeneration could cause to low back pain that trouble lots of the aged people and those who are in intensive labor [3]. There are several factors have been implicated in disc degeneration (Fig. 2). Disc degeneration can be defined as an age-related, cell-mediated molecular degradation process under genetic factor that is accelerated by nutrition, mechanical factors, toxic or metabolic influence [4].

In the degenerative disc, the boundary between NP and AF becomes less clear, NP becomes less gel-like and more fibrous and AF becomes disorganized (Fig. 3). With disc degeneration, proteoglycans of the NP are progressively lost with poor hydrodynamic transfer. Simultaneously, the integrity of the AF is degraded and radial fissures are generated [3]. The CEPs are also affected by the degenerative process accompanying with ossification. As known, the NP is an avascular tissue in the body; the nutrient supply depends on the capillaries of the surrounding tissue, and then diffuses through CEPs into the inner cells. Once degeneration, the regenerative ability of the NP is limited due to the low cell proliferation rate and insufficient nutrient supply [5]. Recent studies indicated that the disc degeneration originates in the NP with loss of cell number, increase in type I collagen, denaturation of type II collagen and loss of proteoglycans. In the degenerated NP, the anabolic and catabolic metabolism of the

ECM could not be kept in balance and altered the response to mechanical loading [6-8].

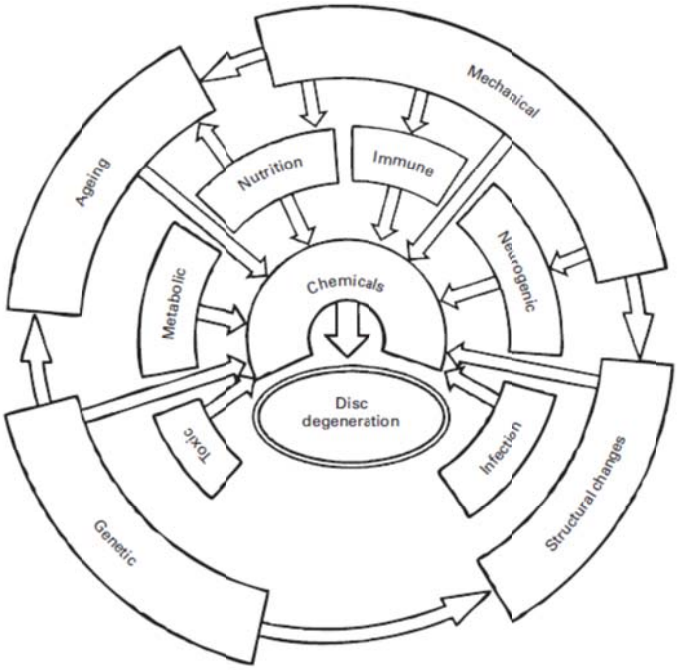

Fig. 1. 3 The pathophysiology of disc degeneration [4]

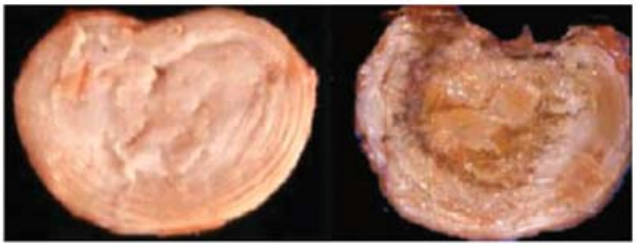

Fig. 1. 4 The normal IVD (left) and degenerative IVD (right) [1]

1.3 Current treatment options for disc degeneration

Disc degeneration is strongly associated with back pain and herniation which results in an increase in health care costs. Disc degeneration could be divided into 5 stages according to the Thompson's classification (Table 1.1). In the first and second stage, there are no significant symptoms but can be traced by magnetic resonance imaging (MRI). Because of the decreased water content in the NP, the T2-weighted MRI signal of the disc changes dramatically from a bright to a gray signal. Generally, no aggressive treatment will be processed in the clinics [9]. In the later stage, disc degeneration may cause low back pain because herniated NP may compress the nerve root. Current clinical treatments for disc degeneration include medication, physical therapy, fusion, artificial disc replacement and discectomy. Whenever possible, doctors prefer treatment other than surgery. For patients who serve pain despite prolonged non-surgical treatment, surgical intervention will be considered. However, these treatments attempt to relieve pain rather than repair the degenerative disc [10-11]. Novel biological treatments are under investigation to treat degenerative disc in the early stages of degenerative process by promoting synthesis or inhibiting degradation of ECM, which have gained more attention in recent years [12-13]. Biological therapy strategies for disc degeneration include protein injection, therapeutic gene transfer and cell-based

therapy. Direct injection of growth factors or cytokine inhibitors may present for a short period of time that may only treat degenerative disc for short term. Therapeutic gene transfer is an approach to maintain high-level expression of growth factor in the target tissue [14-15]. In gene therapy, therapeutic gene is introduced into target cells which can continue to produce the desired ECM. There are two common methods of gene therapy which are in-vivo (direct) and ex-vivo (indirect) gene transfer. In vivo gene therapy introduces vectors containing therapeutic gene directly into the degenerative disc. In the ex-vivo method, therapeutic gene is transferred into cells which are harvested from body and then inject these cells into the target tissue [16]. However, the cell density in the normal disc is low that result in the low efficiency of gene therapy for disc degeneration. To overcome this limitation, cell-based therapy is an approach to transplant new cells in the degenerative disc that can combine with growth factor and scaffold to provide the long-term treatment for disc degeneration [14-15].

Table 1. 1 Thompson grade in the degenerative disc [17]

Grade	Nucleus	Anulus	End-plate	Vertebral body
I	Bulging gel	Discrete fibrous lamellas	Hyaline, uniformly thick	Margins rounded
II	White fibrous tissue peripherally	Mucinous material between lamellas	Thickness irregular	Margins pointed
III	Consolidated fibrous tissue	Extensive mucinous infiltration; loss of anular-nuclear demarcation	Focal defects in cartilage	Early chondrophytes or osteophytes at margins
IV	Horizontal clefts parallel to end-plate	Focal disruptions	Fibrocartilage extending from subchondral bone; irregularity and focal sclerosis in subchondral bone	Osteophytes less than 2 mm
V	Clefts extend through nucleus and anulus		Diffuse sclerosis	Osteophytes greater than 2 mm

CHAPTER 2 THEORETICAL BASIS

2.1 The pathophysiology of disc degeneration

In the normal disc, there is a balance between matrix synthesis and degradation. In the degenerative disc, the homeostasis balance becomes disrupted, leading to diminished synthesis of disc matrix protein and increased expression of catabolic enzymes and inflammatory mediators [18]. Disc degeneration is generally believed that originate in the NP with decrease of cell number, decrease of type II collagen and loss of proteoglycans. In the degenerative NP, cells may lose their phenotype and change extracellular matrix (ECM) composition by decreasing anabolism or increasing catabolism [3, 8]. It has been suggested that degenerative process is accelerated by catabolic factors such as matrix metalloproteinases (MMPs), pro-inflammatory mediators and apoptotic factors. The MMP family degrades at least one component of ECM and can be divided into four main subfamilies: collagenase, stromelysins, gelatinases and membrane metalloproteinases. Collagenases (MMP-1, MMP-8 and MMP-13) degrade the collagen type I, II and III. Stromelysins (MMP-3) degrade many components including proteoglycans, laminin, fibronectin, gelatin, and Type II, III, IV and V collagne. Gelatinases (MMP-2 and MMP-9) cleave several substrates, including gelatins, Type IV, V, VII, X and XI collagen, fibronectin, elastin and proteoglycans.

Tissue inhibitors of metalloproteinases (TIMPs) specifically inhibit active forms of MMPs. TIMP-1 specifically inhibits the activity MMP-3. The imbalance between MMP-3 and TIMP-1 is strongly associated with disc degeneration that is attracting research attention [2, 19-20].

It is well known that IVDs which cause low back pain secrete high level of pro-inflammatory cytokines, such as tumor necrosis factor-α (TNF-α), interleukin-1 (IL-1), inducible nitric oxide synthase (iNOS) and reactive oxygen species (ROS) that promote the production of MMPs and then inhibit the synthesis of the matrix []. Disc cells can be stimulated by IL-1 into increasing their synthesis of MMPs, NO and IL-6 [1997]. The activity of MMP-3 can be enhanced by IL-1 and TIMP-1 production can be decreased by IL-6 that can accelerate degenerative process [19-20].

Anabolic factors, such as insulin-like growth factor (IGF), bone morphogenic protein (BMP) and transforming growth factor (TGF) have been widely studied in recent years (Table 2. 1). Recent studies show that NP cells are capable of producing IGF-1, BMP-7 and TGF-β to promote matrix synthesis. IGF-1 is a single chain polypeptide that can enhance proteoglycan synthesis. BMPs are subfamily of the TGF-β superfamily. BMP-7 that can stimulate NP cells to produce proteoglycans and type II collagen. TGF-β is a multifunctional growth factor that regulates cell growth and matrix

formation [21]. However, the role of TGF-β in the NP remains controversial. More recent studies show that TGF-β is highly expressed in the matrix of degenerated disc and the up-regulation of *TGF-β* might relate to inflammatory reaction. They suggested that the strong expression of *TGF-β* reflects that the disc cells attempt to repair the degraded ECM [22-24]. In addition, it has been shown that ROS can stimulate the expression of *TGF-β* in different types of cells *via* activation of *MMPs* [25-28].

Table 2. 1 The effect of growth factors on disc cells [21]

Factor	Cell Type	Effect	Culture Type	Condition	Dose
IGF-1	Canine NP, AF, TZ	PG synthesis ↑ (NP); cell proliferation ↑ (NP)	Organ culture	Serum (−)	20 ng/mL
IGF-1	Bovine NP	PG synthesis ↑ (NP, AF, TZ); cell proliferation ↑ (NP, TZ)	Monolayer	Serum (−)	1–1000 ng/mL
IGF-1	Bovine NP, AF	PG accumulation ↑		ITS	100 ng/mL
IGF-1	Human IVD (mix)	Apoptosis ↓	Monolayer	1% FCS	50 ng/mL
EGF	Canine NP, AF, TZ	PG synthesis ↑ (NP, AF, TZ); cell proliferation ↑ (NP, AF, TZ)	Organ culture	Serum (−)	1 ng/mL
FGF	Canine NP, AF, TZ	PG synthesis ↑ (NP, AF, TZ); cell proliferation ↑ (NP, AF, TZ)	Organ culture	Serum (−)	300 ng/mL
PDGF	Canine NP, AF, TZ	No effect	Organ culture	Serum (−)	NA
PDGF	Human IVD (mix)	Apoptosis ↓	Monolayer	1% FCS	100 ng/mL
TGF-β1	Rat IVD	Cell viability ↑	Organ culture with endplate	20% FCS	5 ng/mL
TGF-β	Canine NP, AF, TZ	PG synthesis ↑ (NP, AF, TZ); cell proliferation ↑ (NP, TZ)	Organ culture	Serum (−)	1 ng/mL
TGF-β1	Bovine NP, AF	PG accumulation ↑	Collagen/Hyaluronan Scaffold	ITS	10 ng/mL
TGF-β1	Human IVD (mix)	Cell proliferation ↑	Monolayer, Alginate, agarose	1% FCS	0.25–5 ng/mL
TGF-β1	Human IVD (mix)	PG synthesis ↑; cell proliferation ↑	Monolayer	Serum (−)	10 ng/mL
OP-1	Rabbit NP, AF	PG synthesis ↑ (NP, AF); cell proliferation (NP, AF) ↑ Collagen synthesis ↑ (NP, AF); Col II, aggrecan mRNA ↑	Alginate bead	10% FCS	50–200 ng/mL
OP-1	Rabbit NP, AF	After IL-1 treatment, PG accumulation ↑ (NP, AF)	Alginate bead	10% FCS	200 ng/mL
OP-1	Rabbit NP, AF	After C-ABC treatment, PG accumulation ↑ (NP, AF)	Alginate bead	10% FCS	200 ng/mL
OP-1	Bovine NP, AF	PG synthesis ↑ (NP, AF); PG accumulation ↑ (NP, AF)	Alginate bead	10% FCS	200 ng/mL
OP-1	Rabbit IVD	PG content ↑	Organ culture with endplate	10% FCS	200 μg/disc
OP-1	Human NP, AF	PG synthesis ↑ (NP, AF); PG accumulation ↑ (NP, AF)	Alginate bead	10% FCS	200 ng/mL
BMP-2	Rat AF + TZ	GAG, collagen release in media ↑	Monolayer	1% FCS	100–1000 ng/mL
BMP-2	Rabbit AF	GAG, collagen release in media ↑ BMP-6, 7, TGF-β1 mRNA ↑	Monolayer	NA	200 ng/mL
BMP-2	Human IVD (NP + TZ)	PG synthesis ↑; cell proliferation ↑ (NP, TZ) Type I, II, collagen, aggrecan mRNA ↑	Monolayer		>300 ng/mL
BMP-2	Human degenerative IVD	PG synthesis ↑; collagen synthesis ↑	Monolayer	Serum (-)	50–100 ng/mL
BMP-12	Human NP	PG synthesis ↑; collagen synthesis ↑	Monolayer	Serum (-)	25–50 ng/mL

2.2 Reactive oxygen species and oxidative stress

Reactive oxygen species (ROS) are generated by all aerobic cells and is known to participate in a wide variety of molecular and biochemical processes and to directly cause some of the changes observed in cells during differentiation, aging, and transformation [29]. The overproduction of ROS leads to oxidative stress which activates numerous signaling pathways and modulates the function of many enzymes and transcription factors. As known, ROS could be beneficial or detrimental to cell proliferation and differentiation [30]. ROS might be generated as a result of normal intracellular metabolic activity in mitochondria and peroxisomes, as well as from a series of cytosolic enzyme systems. An intricate enzymatic and non-enzymatic antioxidant defense system such as catalase, superoxide mutase, and glutathione peroxidase counteracts regulates overall ROS levels to keep cell in homeostasis. If ROS below the homeostatic set point, it may interrupt the cellular proliferation [31]. Similarly, increased ROS may lead to cell death or to senescence. Generally, the impairment caused by increased ROS is thought to result from random damage to proteins, lipids and nucleus acids. In addition, a rise in ROS levels might induce a stress signal that activates specific redox-sensitive signaling pathways [32-33]. Major signaling pathways activated in response to oxidative stress include nuclear

factor-kappa B (NF-κB), heat-shock transcription factor 1 (HSF1), PI(3)K/Akt, mitogen-activated protein (MAP) kinase and p53 (Fig. 2. 1) [31-33].

The overproduction of ROS led to oxidative stress are commonly associated with apoptosis and senescence of the NP cells that plays an important role to the decrease in number of NP cell during degeneration; moreover, senescent cells may lose their phenotype to produce inadequate ECM in degenerated disc [34-36].

Apoptosis can be initiated *via* extrinsic (mitochondrial-independent) or intrinsic (mitochondrial-dependent) pathway which depends on apoptotic stimuli [37]. Extrinsic pathway is initiated by binding of specific protein ligand (TNF-α superfamily) to the cell surface receptor that can induce the recruitment of fas-associated protein with death domain (FADD) and procaspase-8 into death-inducing signaling complex (DISC). Activation of caspase-8 leads to activation of caspase-3 which results in the apoptosis. The ROS-mediated apoptosis is through the intrinsic pathway, which results in the release of cytochrome c from mitochondria. The complex of cytochrome apoptotic protease activating factor-1 (c-Apaf-1) activates the procaspase-9 which leads to activation of caspase-3 (Fig 2.2). The intrinsic pathway can also be activated *via* the extrinsic Type II pathway through caspase 8-mediated cleavage of the inactive cytosolic protein Bid. Once activated, truncated-Bid (t-Bid) translocates to the mitochondria

where it stimulates cytochrome c release. The activation of caspase-3 in both intrinsic and extrinsic pathways cleaves various cellular substrates that results in morphologic changes in cells and nuclei associated with apoptosis. Both apoptotic pathways have been found to occur in degenerative disc, with static mechanical loading-induced degeneration being mediated *via* intrinsic pathway and disc herniation being mediated *via* extrinsic pathway [38-41].

Cell senescence occurs when normal cells stop dividing. It has been suggested that cell senescence plays a role in disc degeneration. The senescence state is a response to specific stimulus or signaling pathway, including oxidative stress, DNA damage, telomere uncapping, and oncogene activation etc. There are two common signaling pathways of senescence. In the p16-pRB pathway, senescence stimuli activate p16 which lead to activation of pRB. In the p53-p21-pRB pathway, senescence stimuli activate p53, which then induce senescence by activation of pRB through p21. Senescent NP cells may alter gene expression and decrease cell renewal that compromise tissue homeostasis and function (Fig. 2. 3). Recent studies indicated that p53-p21-pRB pathway play a more important role than p16-pRB pathway; moreover, the p53-p21-pRB pathway is reversible. Therefore, prevention of senescence of NP cells can be novel treatment for disc degeneration [32, 34-35].

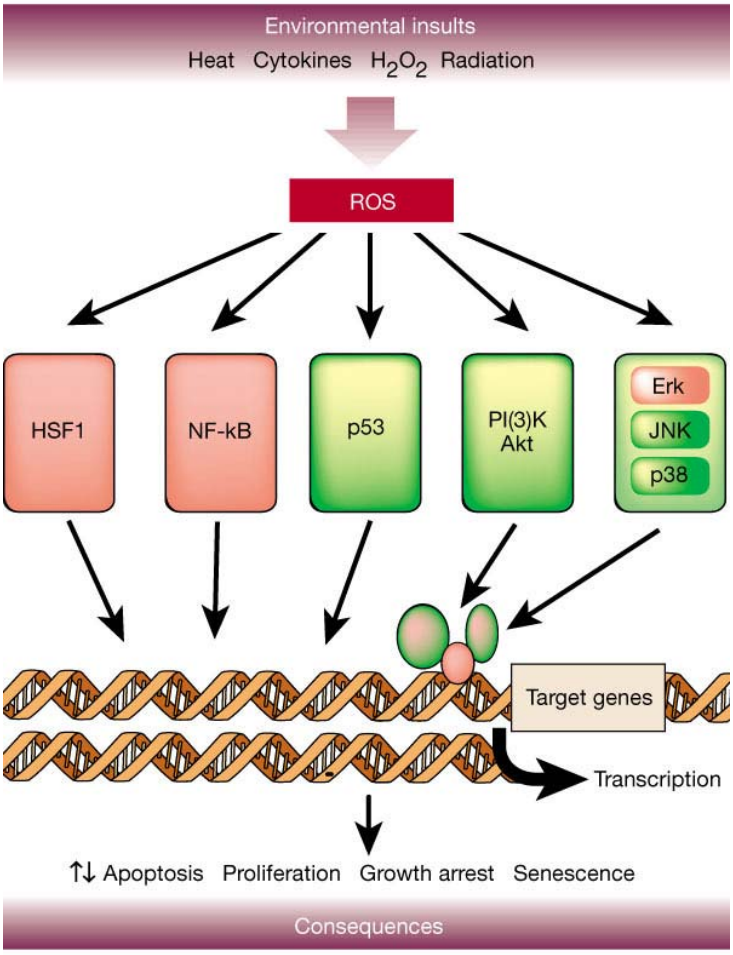

Fig. 2. 1 Major signaling pathways activated in response to oxidative stress [31]

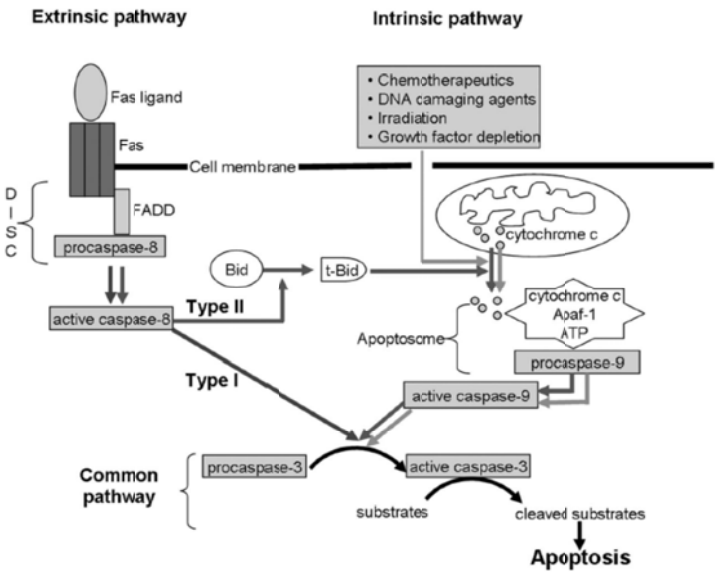

Fig. 2. 2 Components of caspase-dependent intrinsic and extrinsic apoptosis pathways [31]

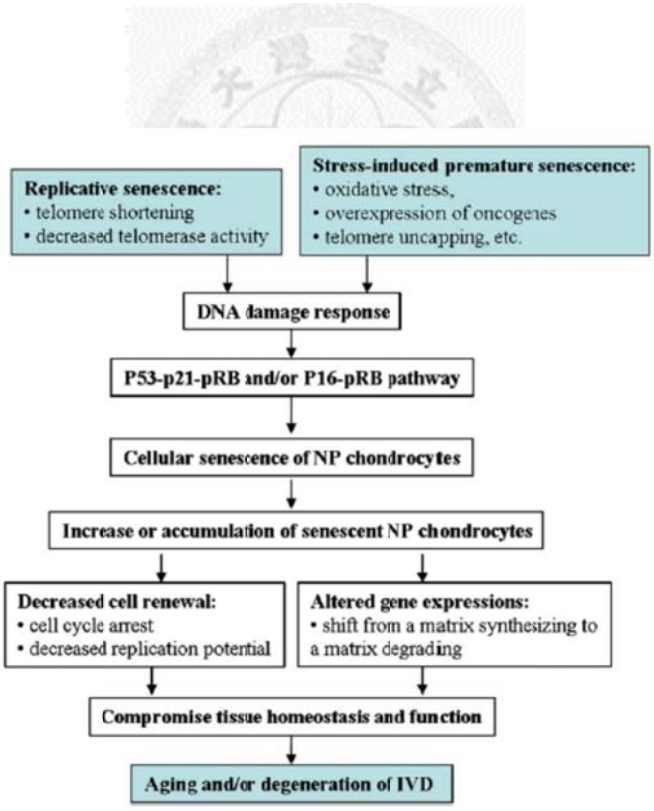

Fig. 2. 3 The hypothetical model for NP cell senescence in degenerative disc [34]

2.3 Polyphenol: ferulic acid

Polyphenols are naturally occurring compounds found largely in the fruits and vegetables. Polyphenols are classified on the basis of the number of phenol rings they contained and of the structural elements binding these rings to one another. They have several hydroxyl groups on aromatic ring(s) and are commonly dived in four classes including phenolic acids, flavonoids, stilbenes and lignans. Ferulic acid (4-hydroxy-3-methoxy cinnamic acid) (FA) is a phenolic acid most abundant in vegetables, especially in eggplants and maize bran [42]. FA possesses the resonance structure and has been found to be an excellent antioxidant (Fig. 2. 4). The mechanism of antioxidant action of FA is that phenolic nucleus and unsaturated side chain of FA can form a resonance stabilized phenoxy radical. Phenoxy radical is highly resonance stabilized since the unpaired electron may be present not only on the oxygen but also it can be delocalized across the entire molecule. This phenoxy radical is unable to initiate a radical chain reaction, and the most probable fate of phenoxy radical is a condensation with another ferulate radical to yield the dimmer curcumin (Fig. 2. 5). Such coupling may lead to a host product, all of which still contain phenolic hydroxyl groups capable of radical scavenging [43-44].

The anti-inflammatory effect of FA has been demonstrated in recent years. FA

decreases the level of inflammatory mediators including ROS, NO and prostaglandin E_2. Oxidative stress induced inflammation is mediated by NF-κB activation, MAP kinases and affect a wide variety of cellular signaling processes leading to generation of inflammatory mediators such as IL-1b, IL-8, TNFα and iNOS and chromatin remodeling (Fig. 2. 6). Polyphenol family inhibits pro-inflammatory gene expression *via* inhibition of IκB, thus inhibiting NF-κB transactivation, as well as restoring transrepressive pathways through the activation of histone deacetylases [45].

FA has been proven to have ability to prevent ROS-induced diseases and to have protective effect on hydroxyl radical oxidation in neuronal cells [46], nicotine-induced DNA damage in blood lymphocytes [47], UV-induced oxidative stress in human lymphocytes [48], γ-radiation induced DNA damage [49] and lipid peroxidation in rat hepatocytes [50].

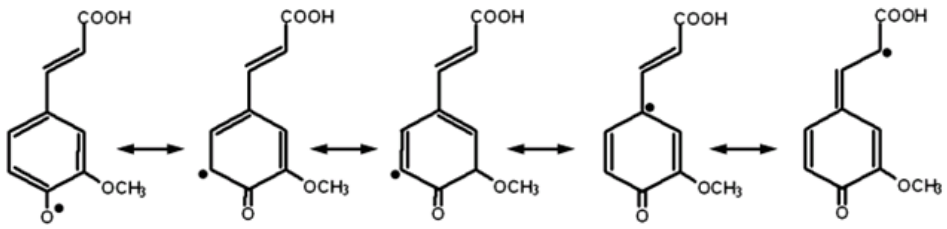

Fig. 2. 4 Resonance structure of FA [43]

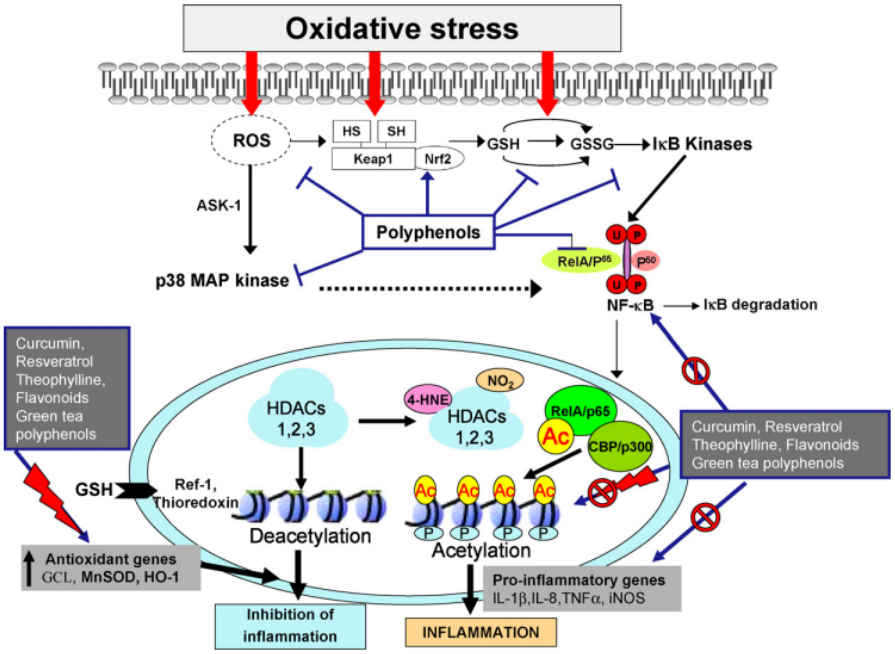

Fig. 2. 5 A schematic model for polyphenols and flavonoids mediated modulation of cell signaling [45]

2.4 *In situ* forming hydrogel

In the past few years, in situ-forming hydrogel have be widely studied for biomedical application. The mechanism of in situ-forming hydrogel formation includes solvent-exchange, UV-irradiation, ionic cross-linkage, pH change and temperature response. Thermosensitive hydrogel formation by simple sol-gel transition and without organic crosslinking agents has been increasing interest in a wide range of biomedical and pharmaceutical applications [51-52].

Chitosan-based thermosensitive hydrogel is currently a great deal of interest for drug and protein delivery [53-54]. Chitosan is a linear copolymer which composed of D-glucosamine and N-acetyl-D-glucosamine by (1, 4)-linkage (Fig. 2. 6). It is soluble in acid solution and contains free amino groups. Chenite *et al.* [55-57] developed thermosensitive chitosan/β-glycerophosphate (C/GP) system that has been widely used in drug and protein delivery. In the system, the gelation time, gel strength and gelation temperature can be controlled by the GP concentration, chitosan concentration and deacetylation degrees of chitosan [56]. The mechanism of sol/gel transition in the C/GP system includes hydrophobic interaction, hydrogen bonding, electrostatic interaction and molecular chain movement. The effective interactions responsible for the sol/gel transition are multiple and briefly described as follows: (1) the increase of chitosan

interchain hydrogen bonding as a consequence of the reduction of electrostatic repulsion due to the basic GP addition, (2) the electrostatic attraction increased between chitosan and GP *via* the amino- and the phosphate groups, respectively, and (3) the hydrophobic interactions between chitosan and chitosan molecules should be enhanced by the structuring action of glycerol on water [55-57]. Roughley et al. [58] suggested that lack for firm structure of the C/GP hydrogel may not be suitable for cell culture. The gel strength of the C/GP hydrogel could be increased by added other polymers. In our previous study [59], the thermosensitive chitosan/gelatin/glycerol phosphate hydrogel has successfully developed as a cell carrier for nucleus pulposus regeneration. The gelatin molecules were added into the C/GP solution to increase the molecular interactions through which to improve the gel strength and shorten the gelation time. When the gelatin is added in the C/GP solution at low temperature, hydrogen bonds exist not only between the OH group of gelatin and the OH and NH_2 groups of chitosan but also between gelatin and water due to the high hydrophilicity of gelatin. At the same time, the low temperature can also reduce the mobility of chitosan molecules, which further prevents the association of chitosan chains. It is thus a poor conformation or shape to build up a 3D network structure because of the difficulty of creating contacts between the junction chains. When temperature is elevated, the intermolecular hydrogen bonding interactions are reduced and the energized water molecules surrounding the

polymer are removed. The dewatered hydrophobic chitosan chains and gelatin molecules entangled one another. As a result, a gel is formed. This type of thermosensitive gelation has also been observed in other cases [58, 60].Therefore, hydrophobic interactions are assumed to be the main driving force to form the gel consisting of chitosan and gelatin at high temperature.

There are several different approaches to drug incorporation have been developed. Direct addition of drugs to hydrogels can be accomplished by encapsulation. The therapeutic molecules can be allowed to release from hydrogel by diffusion. This method show the easiest way to add drug to the hydrogel, however, typical release profiles show the burst release of the drug. The addition of therapeutic molecules before or after cross-linking of polymer can influence the release profile [61]. Incorporation of drug in another release system within hydrogel provides the way to prolong the period of release. Therapeutic molecules can be encapsulated in the microsphere within hydrogel. After hydrogel degradation, the therapeutic molecules are sustained release from hydrogel. Drug delivery system *via* covalent bond between drug and polymer can significantly prolong the period of release compared with the direct incorporation [61]. Covalent attached therapeutic molecules are released from hydrogels due to degradation of hydrogel. In recent years, there are three major drug loading strategies for

chitosan-based hydrogel: permeation, entrapment and covalent bonding (Fig. 2. 10). Both permeation and entrapment method allow the therapeutic molecules release from hydrogel *via* diffusion. The initial burst generally occurs in these two methods due to the gradient concentration formed between hydrogel and surrounding tissue. Covalent bonding between therapeutic molecules and hydrogels may overcome this problem. Covalent bonding method is suitable for hydrophobic drug and can prolong the period of release for several months [61-63].

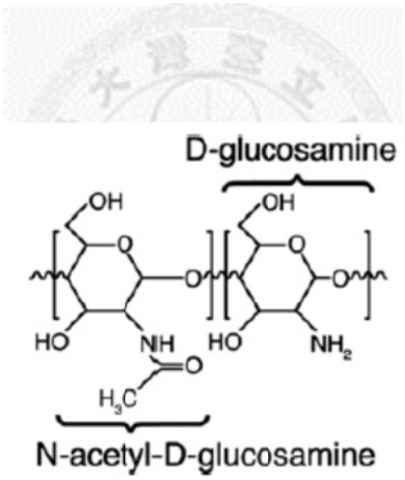

Fig. 2. 6 The structure of chitosan [61]

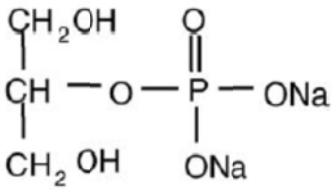

Fig. 2. 7 The structure of β-glycerol phosphate disodium salt hydrate [64]

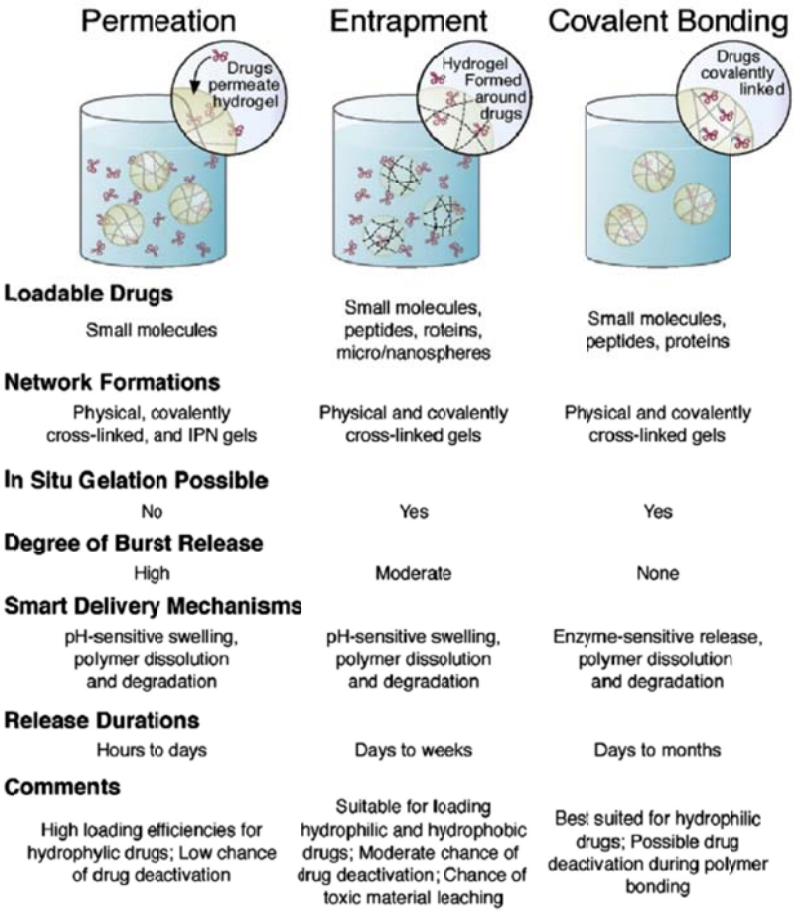

Fig. 2. 8 Three major approaches of drug loading for chitosan hydrogel [61]

2.5 The purpose of study

The object of the study was to evaluate the effects of FA on H_2O_2-induced oxidative stress NP cells. The safety concentration of FA on NP cells was used for further study. The feasibility of use the thermosensitive chitosan/gelatin/ β-glycerophosphate (C/G/GP) hydrogel as a controlled release system of FA for NP regeneration was elucidated. Then we developed the thermosensitive FA-immobilized C/G/GP hydrogel *via* *N*-(3-dimethylaminopropyl)-*N′*-ethylcarbodiimide (EDC) and *N*-hydroxysuccinimide (NHS) crosslinking method. The feasibility of use the thermosensitive FA-immobilized C/G/GP hydrogel as a sustained delivery system for NP regeneration was evaluated.

In the study, the cytotoxicity was evaluated by the water-soluble tetrazolium salt (WST-1), crystal violet and lactate dehydrogenase (LDH) assays. The release profile of FA was performed by ultra violet-visible-near infrared (UV-VIS-NIR) spectrophotometer. The characterization of FA-immobilized C/G/GP hydrogel was analyzed by 2, 4, 6-Trinitrobenzenesulfonic acid solution (TNBS) assay and rheometer. The expression of ECM related gene (*type I collagen*, *type II collagen* and *aggrecan*), catabolic gene (*MMP-3*), anti-catabolic gene (*TIMP-1*), anabolic gene (*TGF-β*, *BMP-7* and *IGF-1*) and pro-inflammatory gene (*IL-1* and *iNOS*) were selected to examine the

effect of FA on H_2O_2-damaged NP cells. The cell viability was evaluated by total DNA assay and crystal violet assay. The sulfated glycosaminoglycans (GAGs) content was performed by dimethylmethylene blue (DMMB) assay and alcian blue staining. The apoptosis analysis of the NP cells was evaluated by caspase-3 activity and terminal deoxynucleotidyl transferase dUTP nick end labeling (TUNEL) staining.

CHAPTER 3 MATERIALS AND METHODS

3.1 Isolation of nucleus pulposus cells

The animal study was approved by the Animal Experimentation Ethics Committee of National Taiwan University Hospital. New Zealand rabbits breed from the Animal Research Center, College of Medicine, National Taiwan University were used in this study and maintained in accordance with the guidelines for the care and use of laboratory animals. The nucleus pulposus (NP) cells were harvested from the IVD of 4 month olds New Zealand rabbits with body weight approximately 2 kg, which were scarified by overdose ketamine hydrochloride injection. The IVD were separated from the rest of tissue and directly dissected to harvest NP. The NP were firstly treated with the 10% penicillin of phosphate buffered saline (PBS) at 37 °C for 10 minutes and and then resuspended in Dulbecco's modified eagle's medium-nutrient mixture F-12 ham medium (DMEM-F12, D8900, Sigma, USA) containing 10% fetal bovine serum (100-106, Gemini Bio-products, USA), 1% penicillin and 0.05% L-Ascorbic acid (A5960, Sigma, USA) with 0.2% collagenase (C0130, Sigma, USA) at 37 °C for 18 hours. NP cells were collected and cultured in DMEM-F12.

3.2 Cytotoxicity of ferulic acid on nucleus pulposus cells

Cytotoxicity of ferulic acid (FA) on nucleus pulposus (NP) cells was performed by the WST-1 (Cell Proliferation Reagent WST-1, Roche, Germany), crystal violet (C3886, Sigma, USA) and lactate dehydrogenase assay (LDH, CytoTox96 Non-Radioactive Cytotoxicity Assay, Promega, USA). The procedures were briefly described as follows. FA was dissolved in dimethyl sulfoxide (DMSO, D2438, Sigma, USA) and added to DMEM-F12 until final concentration of 0.1 M; that would be used as a stock solution. NP cells were seeded on the 96-well cell culture plates (92096, TPP, USA) with the density of 5000 cells per well and cultured in DMEM-F12. After incubated for 18 hours, cells were washed with PBS; the 5 μM, 50 μM, 500 μM and 5000 μM of FA (46280, Fluka, USA) in DMEM-F12 were then separately added to the culture well (200 μl per well) as culture medium throughout the culture. The groups of NP cells cultured in 5 μM, 50 μM, 500 μM and 5000 μM of FA would be abbreviated as FA5, FA50, FA500, and FA5000, respectively. WST-1 was measured on day 1 and day 3 to evaluate the cell viability. The absorbance was measured at 450 nm by the enzyme-linked immunosorbent assay reader (ELISA, Sunrise remote, TECAN, USA).

Crystal violet assay was used to evaluate the cell number. Crystal violet was dissolved in the 10% (volume percent) ethanol (E7148, Sigma, USA). On day 1 and day

3, cells were washed with PBS, and 50 μl of 0.2% (weight percent) crystal solution was added in the culture well for 10 minutes. The crystal violet dye was carefully washed in running water, and then the 100 μl of 33% (volume percent) acetic acid was added in the dry well. The absorbance was measured by the ELISA reader at the wavelength of 570 nm.

LDH assay was used to evaluate the cytotoxicity of FA on NP cells. Released LDH in culture supernatant was measured with a 30-minute coupled enzymatic assay and measured by the ELISA reader at the wavelength of 490 nm. The percentage of cytotoxicity was calculated by the following equation:

$$Cytotoxicity\ (\%) = \frac{OD_{exp} - OD_{medium}}{OD_{total\ lysis} - OD_{medium}} \times 100 \quad \text{..... (1)}$$

3.3 Chemiluminescence assay for reactive oxygen species production

The effective concentration of FA for 100 μM H_2O_2 induced oxidative stress was determined by chemiluminescence (CL) assay using 0.2 mM of luminol (09253, Fluka, USA). The CL measurement was performed by Multi Luminescence Spectrometer (Tohoku Electronic Industrial Co., Ltd, Japan). Oxidative stress was induced by 100 μM H_2O_2 and the 0.5 μM, 1 μM, 5 μM, 50 μM and 500 μM of FA were then separately added to the 35 mm culture dish (T2881-6, Greiner, USA). The sample without treatment was abbreviated as Control group. 100 μM H_2O_2 induced oxidative stress without FA further treatment was designed and abbreviated as H100 group. Oxidative stress was induced by 100 μM H_2O_2 and then further treated with 0.5 μM, 1 μM, 5 μM, 50 μM and 500 μM of FA would be abbreviated as H100FA0.5, H100FA1, H100FA5, H100FA50 and H100FA500, respectively. The culture dish was placed in chamber of spectrometer for background measurement for 50 sec and 1 ml of luminol was then added. The result of reactive oxygen species (ROS) production was expressed as CL counts.

3.4 The effects of ferulic acid on hydrogen peroxide-induced oxidative stress nucleus pulposus cells

3.4.1 Induction of oxidative stress and ferulic acid treatment

The NP cells were seeded in the 6-well cell culture plates with the density of 10^5 cells per well and cultured in DMEM-F12. After incubated for 18 hours, cells were washed with PBS, oxidative stress on NP cells was induced by H_2O_2 (1275, RDH, USA). The NP cells treated with 100 μM H_2O_2 for 30 minutes without FA further treatment was designed and abbreviated as H100 group. The NP cells with 100 μM H_2O_2 for 30 minutes and then further treated with 500 μM FA for 2 hours was designed and abbreviated as H100FA500 group.

3.4.2 RNA extraction and gene expression

The NP cells were collected and total RNA was extracted by RNeasy Protect Mini kit (74104, QIAGEN, Germany). Total RNA yield was quantified by the spectrophotometer at the wavelength of 260 and 280 nm. The ratio of 260 to 280 nm was between 1.6 and 2.0. RNA was treated in RNase-free water and stored in -80 °C for RT-PCR assay. The complementary DNA (cDNA) was synthesized from RNA and

SuperScript^{TM} III First-Strand Synthesis System (18080-051 Invitrogen, USA) for reverse transcription polymerase chain reaction (RT-PCR, PTC-200, MJ Research, USA). In the first-Strand complementary DNA Synthesis, the RNA mixture of 1 μl of 50 ng per μl random hexamers, 1 μl of 10 mM dNTP mix and 8 μl of total RNA was incubated to 65 °C for 5 minutes. The mixture was then kept in ice for 2 minutes. The primer mixture was composed of 2 μl of 10X RT buffer, 4 μl of 25 mM $MgCl_2$, 2 μl of 0.1 M DTT, 1 μl of 40 U per μl RNaseOUT and 1 μl of 200 U per μl SuperScript III. The primer mixture was added to 10 μl of RNA mixture. The RNA-primer mixture was incubated at 25 °C for 10 minutes and then incubated at 50°C for 50 minutes. The reaction was terminated at 85°C for 5 minutes. The RNA-primer mixture was kept in ice for 4 minutes, and 1μl of RNase H was added and incubated at 37°C for 20 minutes. The volume of the PCR mixture of single reaction was 20 μl, which included of 1 μl of primer solution, 9 μl of cDNA and 10 μl of 2X TaqMan universal PCR master mix (4304437, ABI, USA). The target genes of real-time PCR are listed in Table 1. Reaction was performed by ABI PRISM 7700 sequence detection system and ABI PRISM 7700 sequence detection software 1.9.1. The glyceraldehyde-3-phosphate dehydrogenase (*GAPDH*) was used as endogenous housekeeping gene. The relative expression of each target gene was examined by $2^{-\Delta\Delta Ct}$ method.

3.4.3 Total DNA quantification

At the end of 3-day culture, NP cells were collected and total DNA was purified by use of the DNeasy Blood and Tissue kit (69504, QIAGEN, Germany). DNA yield was quantified by ultra violet-visible-near infrared (UV-VIS-NIR) spectrophotometer (DU 7500, Beckman, USA) at the wavelength of 260 nm.

3.4.4 Caspase-3 activity

CaspACE assay (G7220, Promega, USA) was used to evaluate the caspase-3 activity. At the end of 1-day culture, 30 μg of total protein of each sample was added to reaction buffer (32 μl of caspase assay buffer, 2 μl of DMSO and 10 μl of 100 mM DTT), and 2 μl of DEVD-pNA was then added in a 96-well microplate. After reacted for 6 hours at 37 ºC, the buffer was analyzed by ELISA reader at 405 nm for pNA measurement. The amount of pNA is directly proportional to the concentration of caspase-3 which was calculated by the calibration curve of pNA.

3.4.5 TUNEL staining

TUNEL staining (S7111, Chemicon, USA) was used to detect apoptotic nuclei. NP cells was seeded in the 4-well chamber slides (154526, Lab-Tek II, USA) at the density of 5 x 10^4 cells per well for further induction of oxidative stress and post-treatment of FA. After incubation for 1 day, the slides were washed in 2 changes of PBS and fixed in 4% paraformaldehyde solution for 10 minutes and washed in 2 changes of PBS. The equilibration buffer was added for 10 seconds and working strength TdT enzyme solution (77 µl reaction buffer and 33 µl TdT enzyme) was added for 1 hour at 37 ºC. The slides were immersed in stop buffer (1 ml stop buffer and 34 ml distilled de-ionized water) for 10 minutes at room temperature and washed in 3 changes of PBS and then incubated with working strength anti-digoxigenin conjugate solution (68 µl blocking solution and 62 µl anti-digoxigenin conjugate solution) for 30 minutes at room temperature and washed in 4 changes of PBS.

3.5 Thermosensitive chitosan/gelatin/β-glycerol phosphate (C/G/GP) hydrogel as a controlled release system of ferulic acid (FA) for nucleus pulposus regeneration

3.5.1 Preparation of thermosensitive C/G/GP hydrogel

2.5% chitosan (degree of deacetylation > 95%, molecular weights ≒ 340,000, Kiotek, Taiwan) with 1%, 1.5% or 2% gelatin (G1890, Sigma, USA) were dissolved in 0.1 M acetic acid (242853, Sigma, USA) and sterilized by autoclave. Glycerol 2-phosphate disodium salt hydrate (β-GP, G6251, Sigma, USA) was dissolved in deionized water (0.8 w/v) and filtered by 0.22 μm filter (Millex-GV, Millipore, USA) for sterilization. The β-GP solution was added into the chitosan/gelatin solution dropwise under stirring and adjusted the pH value to 7.4. The C/G/GP solution was stored at 4°C and utilized as a cell carrier for the further study.

3.5.2 Reheological characterization

Gelation temperature, gelation time and gel strength were measured by HAAKE RheoStress 600 rheometer equipped with parallel plate sensor (PP35 Ti) in oscillatory mode. The storage (elastic) modulus G' and loss (viscous) modulus G'' versus temperature were measured at a gap of 0.105 mm and the frequency of 1.0 Hz. The temperature at the cross point of G' and G'' was defined as gelation temperature.

3.5.3 *In vitro* FA release study

Five hundred μM of FA-incorporated C/G/GP solution were added to the transwell (200 μl per well) mounted on 24-well plates, and 1.5 ml of PBS was added in each well and then incubated at 37 °C. The 1.5 ml of PBS was collected and 1.5 ml of fresh PBS was then replenished at each time (0.5, 1, 2, 6, 24 and 48 hours). According to the absorption curve of FA, the FA content of the each sample was analyzed by ultra violet-visible-near infrared (UV-VIS-NIR) spectrophotometer (DU 7500, Beckman, USA) at the wavelength of 343 nm. The standard curve of FA was constructed at the wavelength of 343 nm. The FA concentration of each sample was determined by using a linear standard curve.

3.5.4 Induction of oxidative stress and FA treatment

The NP cells were seeded in the 24-well cell culture plates with the density of 5 x 10^4 cells per well and cultured in DMEM-F12. After incubated for 18 hours, cells were washed with PBS, oxidative stress on NP cells was induced by 100 μM H_2O_2 (1275, RDH, USA) for 30 minutes. FA (46280, Fluka, USA) was dissolved in dimethyl sulfoxide (DMSO) (D2438, Sigma, USA) with final concentration of 0.5 M that would be used as a stock solution. The C/G/GP solution was added to the transwell (200 μl per well) mounted on 24-well plates (3413, Corning, USA) incubated with 100 μM H_2O_2-induced oxidative stress NP cells and 1.5 ml of DMEM-F12 was added in each well and then cultured at 37 °C. Based on the cytotoxicity test of FA on NP cells, we have found that the 500 μM of FA might be the threshold to treat NP cells without cytotoxicity. The 100 μM H_2O_2-induced oxidative stress NP cells without and with 500 μM of FA in the C/G/GP hydrogel were abbreviated as Gel and Gel-FA group, respectively.

3.5.5 RNA extraction and gene expression

The NP cells were collected and total RNA was extracted using RNeasy protect mini kit (74104, QIAGEN, Germany). Total RNA yield was detected by the spectrophotometer at 260 and 280 nm. RNA was stored in -80 °C for reverse transcription polymerase chain reaction (RT-PCR). The first strand complementary DNA (cDNA) was synthesized from RNA and SuperScript^{TM} III first-strand synthesis system (18080-051 Invitrogen, USA) for RT-PCR (PTC-200, MJ Research, USA) according to the instructions provided by the manufacturer. The volume of the PCR mixture of single reaction was 20 μl containing 1 μl of primer solution, 9 μl of cDNA and 10 μl of 2X TaqMan universal PCR master mix (4304437, ABI, USA). The target genes of real-time PCR are summarized in Table 1. Reaction was performed by ABI PRISM 7700 Sequence detection system and ABI PRISM 7700 sequence detection software 1.9.1. The target genes were normalized to the glyceraldehyde-3-phosphate dehydrogenase (GAPDH). The relative mRNA expression of each target gene was determined using $^{\Delta\Delta}$Ct method.

3.5.6 Total DNA quantification

At the end of 1-day culture, NP cells were collected and total DNA was purified by use of the DNeasy blood and tissue kit (69504, QIAGEN, Germany) following the instructions provided by the manufacturer. Total DNA yield was quantified by ultra violet/visible/near infrared (UV/VIS/NIR) spectrophotometer (DU 7500, Beckman, USA) at the wavelength of 260 and 280 nm. The ratio of 260 to 280 nm was between 1.6 and 2.0.

3.5.7 Sulfated glycosaminoglycan content

The sulfated-glycosaminoglycans (GAGs) production was evaluated by DMMB (341088, Sigma, USA) assay. At the end of 1-day culture, the culture medium of each sample was collected and transferred 40 μl of the supernatant of each sample to a 96-well microplate, and 250 μl of DMMB solution was then added. The DMMB-sulfated GAGs complex product was examined by ELISA reader at the wavelength of 595 nm. The sulfated GAGs content of each sample was determined by using a calibration curve which was performed by condroitin-6-sulfate (C4384, Sigma, USA).

3.5.8 Alcian blue staining

At the end of 1-day culture, cells were washed twice with PBS and fix in 10% neutral buffered formalin (H121-08, Mallinckrodt Analytical, USA) for 30 minutes and then washed twice with PBS. 3% acetic acid was added and then washed in running water for 1 minute. Alcian blue (pH 1.0, Muto pure chemicals, Japan) was added for 30 minutes and cells were then washed in running water for 1 minute. Kernechtrot (Muto pure chemicals, Japan) was added for 5 minutes and then washed in running water for 1 minute. The cells were dehydrated in 2 changes of 95% alcohol and absolute alcohol (459844, Sigma, USA) for 1 minute each.

3.5.9 Caspase-3 activity

At the end of 1-day culture, caspase-3 activity was analyzed by CaspACE assay system (G7220, Promega, USA) according to the instructions provided by the manufacturer. Briefly, 30 μg of total protein of each sample was added to reaction buffer (32 μl of caspase assay buffer, 2 μl of DMSO and 10 μl of 100 mM DTT), and 2 μl of DEVD-pNA was then added in a 96-well microplate and incubated at 37 ºC for 4 hours. The sample was analyzed by ELISA reader at the wavelength of 405 nm. The optical density (OD) value of each sample was calculated by the calibration curve of

pNA and the concentration of caspase-3 was obtained.

3.5.10 TUNEL staining

Terminal deoxynucleotidyl transferase-mediated dUTP nick end labeling (TUNEL) staining was performed by ApopTag® plus fluorescein *in situ* apoptosis detection kit (S7111, Chemicon, USA). At the end of 1-day culture, cells were washed twice with PBS and fix in 10% neutral buffered formalin (H121-08, Mallinckrodt Analytical, USA) for 30 minutes and then washed twice with PBS. Cells were post-fixed in precooled ethanol/acetic acid (2:1) solution for 5 minutes at -20 °C and then washed twice with PBS. The equilibration buffer was added for 10 seconds and working strength TdT enzyme solution (70% reaction buffer and 30% TdT enzyme) was added for 1 hour at 37 ºC. The stop buffer (1 ml stop buffer and 34 ml distilled de-ionized water) was added for 10 minutes at room temperature and washed in 3 changes of PBS and then incubated with working strength anti-digoxigenin conjugate solution (53% blocking solution and 47% anti-digoxigenin conjugate solution) for 30 minutes at room temperature and washed in 4 changes of PBS.

3.6 The effects of thermosensitive ferulic acid-immobilized chitosan/gelatin/β-glycerol phosphate (FA-immobilized C/G/GP) hydrogel on nucleus pulposus cells under hydrogen peroxide-induced oxidative stress

3.6.1 Preparation of thermosensitive FA-immobilized C/G/GP hydrogel

Ferulic acid (46280, Fluka, USA) was dissolved in dimethyl sulfoxide (DMSO, D2438, Sigma, USA) with concentration of 0.1 M. *N*-(3-dimethylaminopropyl)-*N'*-ethylcarbodiimide (EDC, E1769, Sigma, USA) and *N*-hydroxysuccinimide (NHS, 56480, Fluka, USA) were dissolved in water with concentration of 1 M and 0.25 M respectively. 8% gelatin (G1890, Sigma, USA) and 2.5% chitosan (degree of deacetylation > 95%, molecular weights ≒ 340,000, Kiotek, Taiwan) were dissolved in water and 0.1 M acetic acid (242853, Sigma, USA) respectively. Both gelatin and chitosan solution were sterilized by autoclaving at 121 °C for 30 minutes. FA-immobilized gelatin solution was prepared by mixing 100 μl of 1 M EDC and 400 μl of 0.25 M NHS with 1 ml of 0.01 M FA and vortexed for 1 hour. The mixture was filtered by 0.22 μm filter (Millex-GV, Millipore, USA) for sterilization and then mixed with 1ml of 8% gelatin solution and vortexed for 1 hour. FA-immobilized gelatin solution was then mixed with 2.5% chitosan solution to form the FA-immobilized chitosan-gelatin solution. 44.4% β-glycerophosphate disodium salt

hydrate (β-GP, G5422, Sigma, USA) solution was sterilized by passing through a 0.22 μm filter (Millex-GV, Millipore, USA) and added drop by drop to the FA-immobilized chitosan-gelatin solution under stirring and adjusted the pH value to 7.4. The FA-immobilized C/G/GP solution was stored at 4 °C until further use.

3.6.2 Characterization of FA-immobilized gelatin

The 2, 4, 6-trinitrobenzenesulfonic acid solution (TNBS, P2297, Sigma, USA) assay was used for the detection of primary amino groups. The residual amino group of both gelatin (without immobilization of FA) and FA-immobilized gelatin were analyzed by TNBS assay. 10 μl of sample was mixed with 90 μl of 0.1 M sodium hydroxide (221465, Sigma, USA). The mixture was transferred into a 96-well microplate and reacted with 50 μl of 0.1% TNBS for 2 hours at 37 °C. After 2 hours, 75 μl of stop solution containing 50 μl of 10% SDS (L4522, Sigma, USA) and 25 μl of 1 N HCl was added to terminate the reaction. The optical density (OD) value was measured at 420 nm using an enzyme-linked immunosorbent assay reader (ELISA, Sunrise remote, TECAN, USA). The residual amino group content of sample was determined by using a linear standard curve which was constructed by glycine (G7126, Sigma, USA).

3.6.3 Reheological characterization

Gelation temperature and gelation time of the FA-immobilized C/G/GP hydrogel were measured by HAAKE RheoStress 600 rheometer (Thermo Fisher Scientific Inc., Waltham, MA, USA) equipped with parallel plate sensor (PP35 Ti) in oscillatory mode. The elastic modulus (G') and viscous modulus (G'') versus temperature were measured at a gap of 0.105 mm and the frequency of 1.0 Hz. The gelation temperature and gelation time were defined at which the G' becomes larger than the G".

3.6.4 Cytotoxicity of thermosensitive FA-immobilized C/G/GP hydrogel on NP cells

Cytotoxicity of FA-immobilized C/G/GP hydrogel on NP cells was performed by extraction method. The 0.1 g FA-immobilized C/G/GP hydrogel was immersed in 1 ml DMEM-F12 in a 48-well culture plate at 37 °C. The supernatant from each well was collected on day 3 for cytotoxicity test. NP cells were seeded in 96-well cell culture plates at a density of 5,000 cells per well and cultured in DMEM-F12 for 18 hours. Cells were then cultured in the extraction medium obtained from the developed hydrogel. WST-1 (Cell Proliferation Reagent WST-1, Roche, Germany) and lactate dehydrogenase (LDH, CytoTox96 Non-Radioactive Cytotoxicity Assay, Promega, USA) were used to evaluate the cell viability and cytotoxicity of the developed hydrogel on

NP cells on day 1 and day 3. The OD value of WST-1 and LDH assay were measured at 450 and 490 nm with an ELISA reader respectively. The percentage of cytotoxicity was calculated by the following equation:

$$Cytotoxicity(\%) = \frac{OD_{\exp} - OD_{medium}}{OD_{total\ lysis} - OD_{medium}} \times 100$$

3.6.5 *In vitro* FA release study

Two hundred μl of FA-immobilized C/G/GP solution or C/G/GP (without immobilization of FA) was added to the transwell mounted on 24-well plates (3413, Corning, USA) and 1.5 ml of PBS was then added in each well and incubated at 37 °C. The 1.5 ml of PBS was collected and 1.5 ml of fresh PBS was then added at each time (0.5, 1, 2, 6, 24 and 48 hours). The content of FA was evaluated by ultra violet-visible-near infrared (UV-VIS-NIR) spectrophotometer (DU 7500, Beckman, USA) at the wavelength of 343 nm according to the absorption spectrum of FA. The FA concentration of each sample was calculated from the linear standard curve of FA.

3.6.6 Induction of oxidative stress and FA-immobilized C/G/GP hydrogel treatment

The NP cells were seeded in the 24-well cell culture plates with the density of 5 x 10^4 cells per well and cultured in DMEM-F12. After 18 hours, cells were washed with PBS and 1.5 ml of DMEM-F12 was then added. Oxidative stress on NP cells was induced by 100 μM H_2O_2 (1275, RDH, USA) for 30 minutes. The 200 μl of FA-immobilized C/G/GP or C/G/GP (without immobilization of FA) solution were added to the transwell mounted on 24-well plates incubated with 100 μM H_2O_2-induced oxidative stress NP cells and then cultured at 37 °C. The 100 μM H_2O_2-induced oxidative stress NP cells with C/G/GP hydrogel and with FA-immobilized C/G/GP hydrogel were abbreviated as C/G/GP and FA-immobilized C/G/GP group respectively.

3.6.7 RNA extraction and gene expression

The total RNA was extracted from NP cells using RNeasy protect mini kit (74104, QIAGEN, Germany) after 2.5 hour. The OD ratio (260/280 nm) of each RNA sample was between 1.8 and 2.0. RNA was stored in -80 °C for reverse transcription polymerase chain reaction (RT-PCR). The first strand complementary DNA (cDNA) was synthesized from RNA and SuperScript^{TM} III First-Strand Synthesis System (18080-051, Invitrogen, USA) for RT-PCR (PTC-200, MJ Research, USA) in accordance with the manufacturer's instruction. 1 μl of primer, 9 μl of cDNA and 10 μl of 2X TaqMan universal PCR master mix (4304437, ABI, USA) were mixed in a final volume of 20 μl for single reaction. Reaction was performed by ABI PRISM 7700 sequence detection system and ABI PRISM 7700 sequence detection software 1.9.1. The target genes of real-time PCR reaction were summarized in Table 1 and each target gene was calibrated for glyceraldehyde-3-phosphate dehydrogenase (GAPDH). The relative quantitation value of gene expression was determined using $^{\Delta\Delta}$Ct method.

3.6.8 Analysis of cell numbers

The cell number in each well was evaluated by crystal violet assay (C3886, Sigma, USA) on day 1. Crystal violet was dissolved in the 10% (volume percent) ethanol (E7148, Sigma, USA). NP cells were washed with PBS and 50 μl of 0.2% (weight percent) crystal solution was then added for 10 minutes. The 24-well cell culture plate was washed with running water and the 100 μl of 33% (volume percent) acetic acid was then added. 100 μl of the supernatant of each sample was transferred to a 96-well microplate. The absorbance was measured at the wavelength of 570 nm using an ELISA reader. The cell number of each sample was calculated from the linear standard curve with known numbers of NP cells.

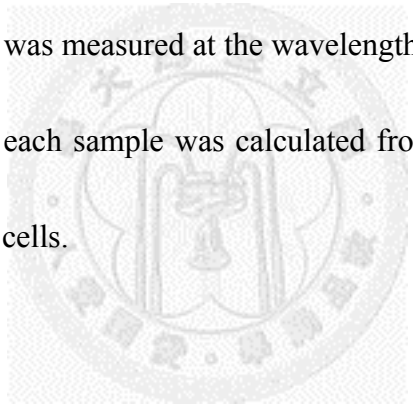

3.6.9 Sulfated glycosaminoglycan content

The sulfated glycosaminoglycan (GAG) content was analyzed by 1, 9-dimethylmethylene blue (DMMB, 341088, Sigma, USA) assay [23]. The culture medium of each well was collected on day 1. 40 μl of each sample was mixed with 250 μl of DMMB solution in a 96-well microplate. The sulfated GAG-DMMB complex was detected by ELISA reader at the wavelength of 595 nm. The sulfated GAG production was calculated form the standard curve which was constructed by condroitin-6-sulfate

(C4384, Sigma, USA).

3.6.10 Caspase-3 activity

NP cells were collected at the end of 1-day culture. Total protein content was determined using BCA protein assay kit (23227, Pierce, USA) according to the manufacturer's instructions. Caspase-3 activity was evaluated by CaspACE assay system (G7220, Promega, USA). 30 μg of total protein of each sample was mixed with a reaction buffer containing 2 μl of DMSO, 10 μl of 100 mM DTT and 32 μl of caspase assay buffer in a 96-well microplate. 2 μl of DEVD-pNA was then added and incubated at 37 ºC for 4 hours. The absorbance was measured at the wavelength of 405 nm using an ELISA reader. The caspase-3 concentration of the sample was calculated by the linear standard curve of pNA.

3.6.11 TUNEL staining

At the end of 1-day culture, terminal deoxynucleotidyl transferase-mediated dUTP nick end labeling (TUNEL) staining was performed by using ApopTag® plus fluorescein *in situ* apoptosis detection kit (S7111, Chemicon, USA) according to the instructions provided by the manufacturer. Briefly, NP cells were washed with PBS and then fixed in 10% neutral buffered formalin (H121-08, Mallinckrodt Analytical, USA) for 30 minutes. Cells were washed with PBS and then post-fixed in acetic acid/ethanol (1:2) solution for 5 minutes at -20 °C. The cells were washed with PBS and the equilibration buffer was added for 10 seconds and working strength TdT enzyme solution containg 70% reaction buffer and 30% TdT enzyme was added for 1 hour at 37 ºC. The stop solution (1 ml stop buffer and 34 ml distilled de-ionized water) was added for 10 minutes at room temperature and washed with PBS. The working strength anti-digoxigenin conjugate solution (53% blocking solution and 47% anti-digoxigenin conjugate solution) was added and incubated for 30 minutes at room temperature and then washed in 4 changes of PBS.

3.7 Statistical analysis

Statistical analysis of WST-1 assay, LDH assay, crystal violet assay, mRNA gene expression, sulfated GAGs content and caspase-3 activity was analyzed by one-way analysis of variance (ANOVA). The results were considered significantly different when the *p*-value was < 0.05.

CHAPTER 4 RESULTS

4.1 Cytotoxicity of ferulic acid on nucleus pulposus cells

The groups of nucleus pulposus (NP) cells cultured in 5 μM, 50 μM, 500 μM and 5000 μM of ferulic acid (FA) would be abbreviated as FA5, FA50, FA500 and FA5000, respectively. Fig. 4. 1(a) showed the results of WST-1 assay that would be in terms of mitochondrial activity. The OD value of FA5000 group showed 0.414 ± 0.026 on day 1 that was significantly lower than that of the control group of 0.594 ± 0.051 ($p < 0.05$). There were no statistically difference of OD value in the other experimental groups (FA5, FA50 and FA500) and control group at the first day. On day 3, the OD value of FA5000 was 0.538 ± 0.005 that was much lower ($p < 0.05$) than that of the control group (1.422 ± 0.113). The OD value of FA500 was 1.686 ± 0.051 that was higher than that of the control group on day 3.

The results of crystal violet assay related with total DNA measurement were shown in Fig. 4. 1(b). The OD value of the control group on day 1 and day 3 were 0.272 ± 0.039 and 0.477 ± 0.052, respectively. The OD value of FA5000 and on day 1 and day 3 were 0.145 ± 0.015 and 0.152 ± 0.017, respectively. From the results, we could tell that the cell number in FA5000 was much lower than the control group on day 1 and day 3.

There is no significant difference in OD value on day1 between control group and FA500. On day 3, the OD value of FA500 was 0.689 ± 0.054 that was higher than the control group of 0.477 ± 0.052 ($p < 0.05$). The OD value of FA 5 and FA50 showed no significant difference with the control group on day 1 and day 3.

The results of LDH analysis were shown in Fig. 4. 1(c) that would be interpreted as the cytotoxicity followed by the calculation of equation (1) in section 3.2. The cytotoxicity of FA5000 was 55.8% and 49.9% on day 1 and day 3, respectively. The cytotoxicity of control group was 35.5% and 27.5% aon day 1 and day 3, respectively. The results showed that the cytotoxicity of FA5000 was higher than that of the control group no matter on day 1 or day 3. There was no significant difference in cytotoxicity between other three groups (FA5, FA50 and FA500) and control group.

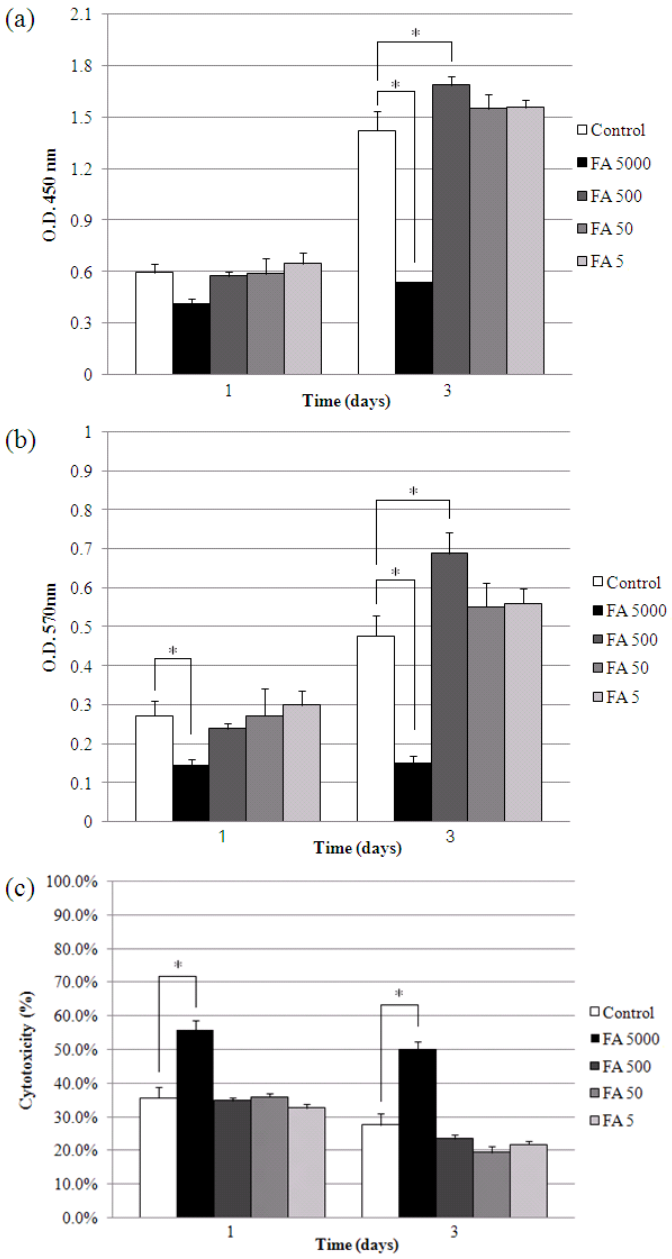

Fig. 4. 1 Cytotoxicity of FA on NP cells was measured on day 1 and day 3. (a) WST-1 assay (n = 4, *, $p < 0.05$), (b) Crystal violet assay (n = 4, *, $p < 0.05$) and (c) LDH assay (n = 4, *, $p < 0.05$). NP cells were cultured with 5 μM, 50 μM, 500 μM and 5000 μM of FA compared individually with normal NP cells (without treatment, Control).

4.2 Reactive oxygen species scavenging effect

As shown in Fig. 4. 2, the result of reactive oxygen species (ROS) production was expressed as CL counts. The ROS level was significantly ($p < 0.05$) increased in H100 group (70.18 ± 18.93) compared with control group (10.07 ± 15.88). The CL counts of H100FA0.5, H100FA1, H100FA5, H100FA50 and H100FA500 were -2.83 ± 11.20, -2.18 ± 16.33, 7.6 ± 6.59, -0.78 ± 11.12 and 2.1 ± 5.51, respectively. The ROS level was dramatically decline in the post-treatment FA groups compare with H100 group individually. There was no significant difference between the control group and post-treatment FA group (H100FA0.5, H100FA1, H100FA5, H100FA50 or H100FA500) in the ROS production.

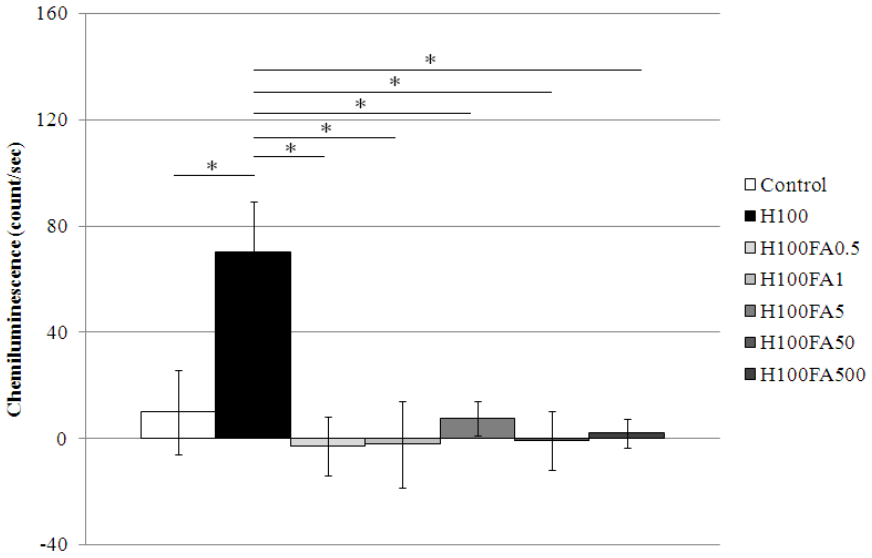

Fig. 4. 2 The ROS scavenging effect of different concentration of FA. Oxidative stress was induced by 100 μM H_2O_2 and then further treated with 0.5 μM, 1 μM, 5 μM, 50 μM and 500 μM of FA would be abbreviated as H100FA0.5, H100FA1, H100FA5, H100FA50 and H100FA500, respectively (n = 3, *, $p < 0.05$).

4.3 The effects of ferulic acid on hydrogen peroxide-induced oxidative stress nucleus pulposus cells

4.3.1 Gene expression

The NP cells treated with 100 μM H_2O_2 for 30 minutes without FA further treatment was designed and abbreviated as H100 group; and the NP cells with 100 μM H_2O_2 for 30 minutes and then further treated with 500 μM FA for 2 hours was designed and abbreviated as H100FA500 group. The fresh NP cells were the control group and the fold would be normalized to 1 for each gene expression that would be compared with those of in H100 group and H100FA500 group.

As shown in Fig. 4. 3, the gene expression of *aggrecan* was significantly down regulated in H100 group with 0.6 folds to the control group. There was no significant difference in *aggrecan* between the control group and H100FA500 group. The expression of *aggrecan* was up regulated in H100FA500 group (1.2106 ± 0.2039) compared with H100 group (0.6034 ± 0.1882). There was no significant difference between the control group and H100 group in the expression of *type II collagen*. The expression of *type II collagen* was up regulated in H100FA500 group with 1.5 folds to the control group. The expression of *type II collagen* was up regulated in H100FA500 group (1.5585 ± 0.2369) compared with H100 group (1.0552 ± 0.1720). There was no

significant difference in *type I collagen* expression between experimental groups (H100 and H100FA500) and control groups.

MMP-3 and *TIMP-1* were generally used to examine the catabolic gene and anti-catabolic gene, respectively. As shown in Fig. 4. 3, the expression of *MMP-3* was up regulated in H100 group with 2.1257 folds to control group. There was no significant difference in the expression of *MMP-3* between the control group and H100FA500 group. The expression of *MMP-3* was down regulated in H100FA500 group (0.8664 ± 0.1357) compared with H100 group (2.1257 ± 0.0183). *TIMP-1* was significantly down regulated in H100 group and H100FA500 group with 0.1342 folds and 0.2406 folds, respectively, to the control group. The expression of *TIMP-1* in H100FA500 group (0.2406 ± 0.0070) was statistically higher than that of H100 group (0.1342 ± 0.0399).

TGF-β, BMP-7 and *IGF-1*were the anabolic related genes. As shown in Fig. 4. 3, the expression of *TGF-β* of H100 group was 1.4626-fold higher than that of control group. There was no significant difference in *TGF-β* expression between H100FA500 group and control group. The expression of *TGF-β* in H100 group (1.4626 ± 0.0551) was higher than that of in H100FA500 group (1.0917 ± 0.0210). There was no significant difference in *BMP-7* expression between H100 group and control group. The expression of *BMP-7* in H100FA500 group showed 1.9395-fold higher than that of in

control group. The expression of *BMP-7* in H100 group showed lower than that of in H100FA500 group. The expression of *IGF-1* was no significant difference for all the groups.

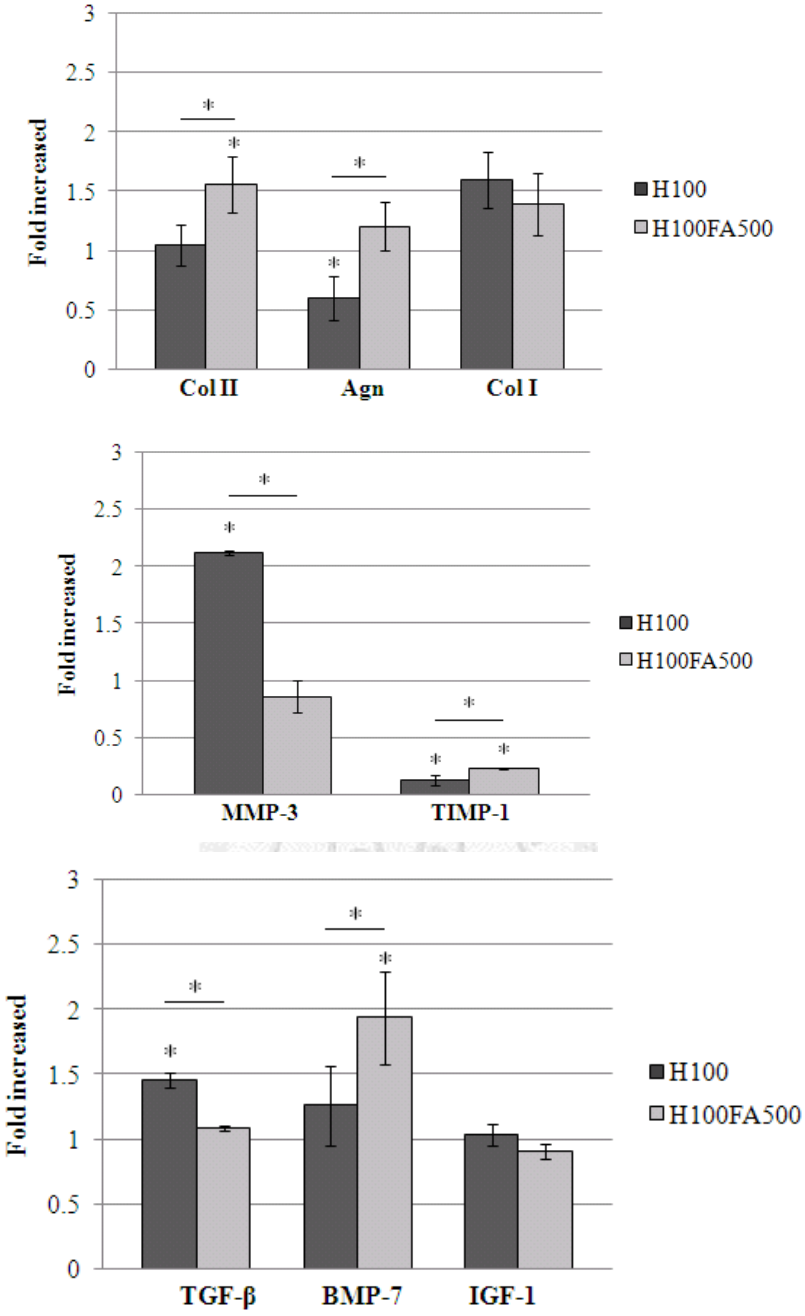

Fig. 4. 3 Gene expression of normal NP cells (without treatment), H_2O_2-induced NP cells (H100) and post-treatment of FA on H_2O_2-induced NP cells (H100FA500). The result was expressed as fold increase compared with normal NP cells. Each target gene was normalized to GAPDH (n = 4, *, $p < 0.05$).

4.3.2 Sulfated glycosaminoglycan production

The sulfated GAGs to DNA ratio was defined as the sulfated GAGs production per NP cell. As shown in Fig. 4. 4, the sulfated GAGs to DNA ratio in the H100 group was 26.122 ± 1.264 that was significantly lower ($p < 0.05$) than the control group (38.652 ± 2.714). There was no significant difference in the ratio between H100FA500 group (40.668 ± 4.560) and control group (38.652 ± 2.714). The ratio in H100FA500 group (40.668 ± 4.560) was higher ($p < 0.05$) than that in H100 group (26.122 ± 1.264).

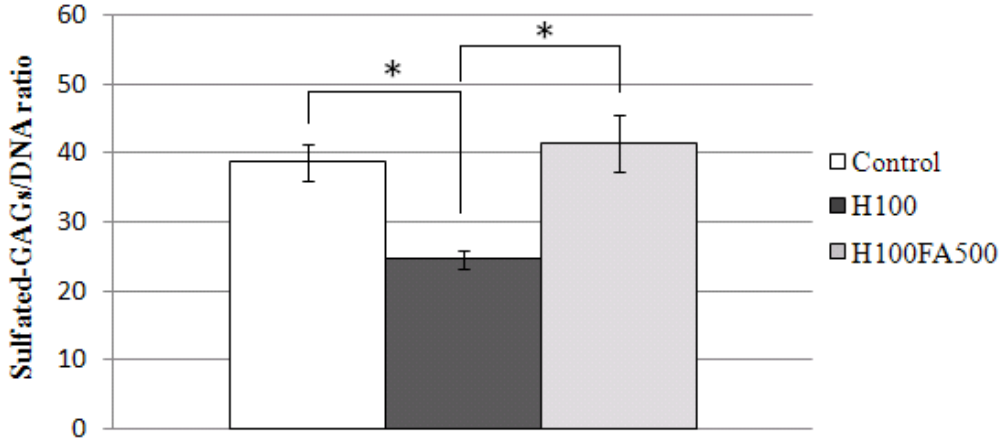

Fig. 4. 4 The ratio of sulfated GAGs to DNA of normal NP cells (without treatment, Control), H_2O_2-induced NP cells (H100) and post-treatment of FA on H_2O_2-induced NP cells (H100FA500) (n = 4,*, $p < 0.05$).

4.3.3 Caspase-3 activity

As shown in Fig. 4. 5, the caspase-3 activity of H100 group was 4.182 ± 0.715 that was much higher ($p < 0.05$) than that of control group (1 ± 0.538). There was no significant difference in caspase-3 activity between H100FA500 group (2.012 ± 0.705) and control group (1 ± 0.538). The caspase-3 activity in H100FA500 group (2.012 ± 0.705) was about 2 times lower ($p < 0.05$) than that of H100 group (4.182 ± 0.715).

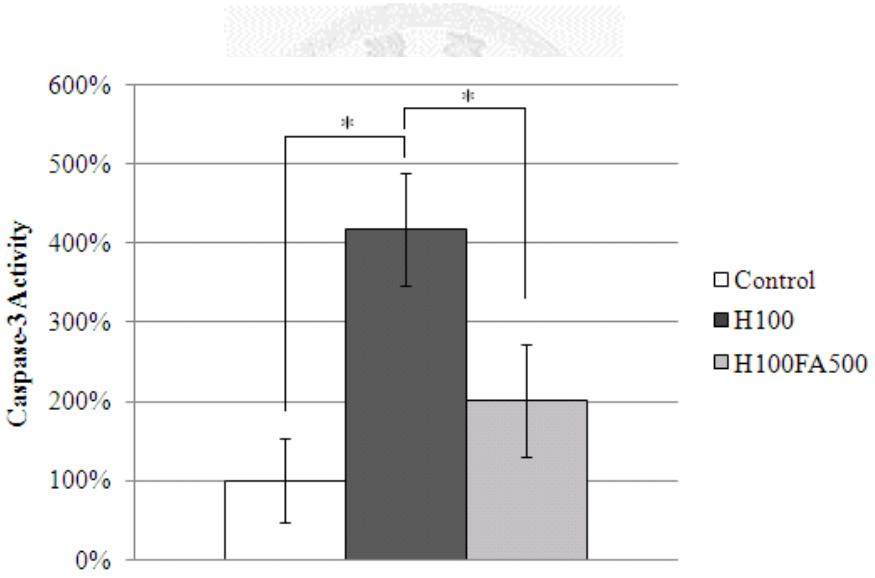

Fig. 4. 5 The caspase-3 activity of normal NP cells (without treatment, Control), H_2O_2-induced NP cells (H100) and post-treatment of FA on H_2O_2-induced NP cells (H100FA500) (n = 4,*, $p < 0.05$).

4.3.4 TUNEL staining

DNA fragmentations are generally happened in the apoptotic cells that can be used for evaluation of the cell apoptosis. TUNEL stain provides a convenient way to detect the cell apoptosis by the way of the specific staining to 3'-OH ends in apoptotic cells; which turn the apoptotic nucleus in green spot.

Fig.4. 6 showed the results of TUNEL stain of control group (Fig. 4. 6(a)), H100 (Fig. 4. 6(b)) and H100FA500 (Fig. 4. 6(c)). As shown in Fig. 4. 6(b), H100 group showed lots of green apoptotic nuclei spots under the examination of confocal microscope. There were only few green apoptotic nucleus spotted in control group and in H100FA500 group.

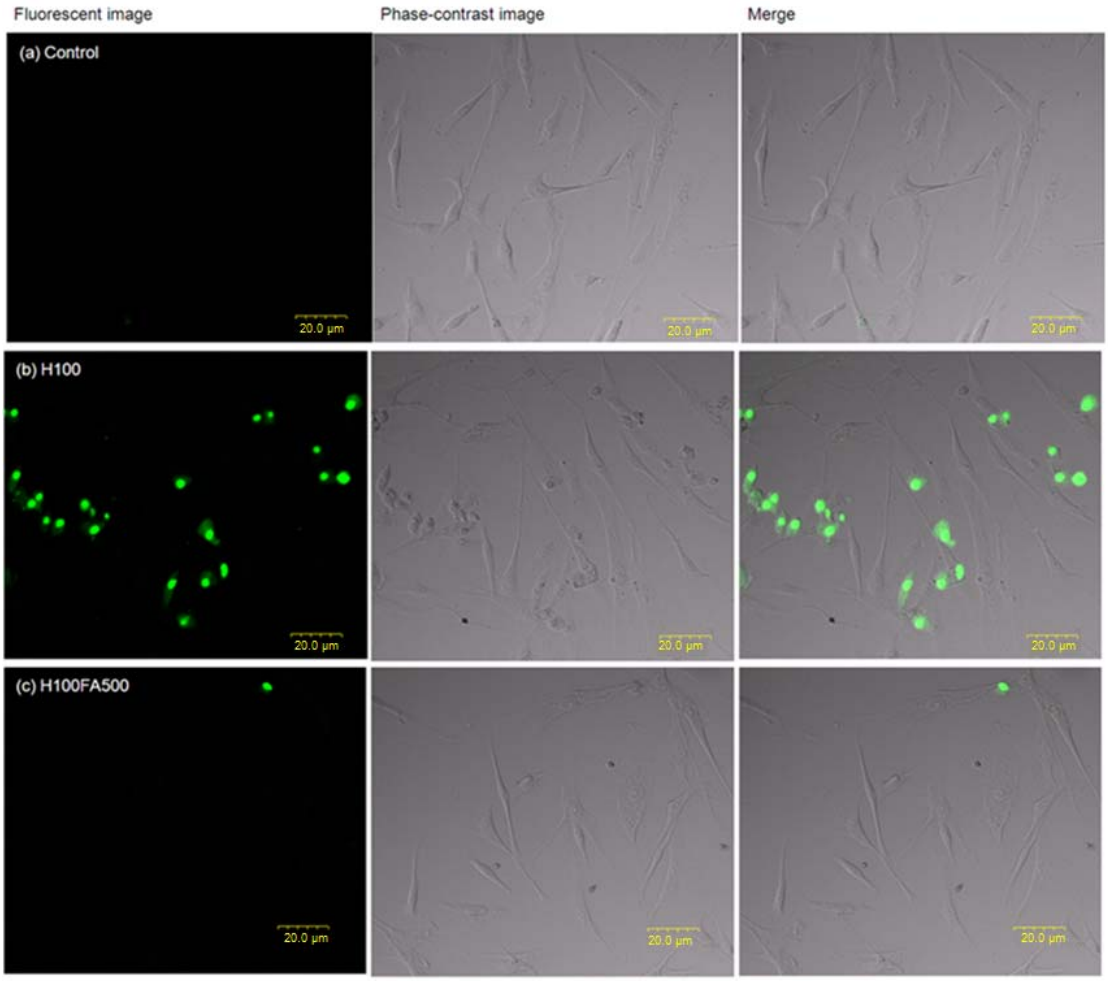

Fig. 4. 6 TUNEL staining of (a) Normal NP cells (without treatment, Control), (b) H_2O_2-induced NP cells (H100) and (c) post-treatment of FA on H_2O_2-induced NP cells (H100FA500).

4.4 Thermosensitive chitosan/gelatin/β-glycerol phosphate (C/G/GP) hydrogel as a controlled release system of ferulic acid for nucleus pulposus regeneration

4.4.1 The release of FA from C/G/GP hydrogel

The release profile of FA from C/G/GP hydrogel was shown in Fig. 4. 7. The cumulative concentration of FA in the PBS at 0.5, 1, 2, 6, 24 and 48 hours were 1.058 ± 0.740, 1.897 ± 0.776, 2.834 ± 0.977, 6.261 ± 1.096, 10.327 ± 1.653 and 11.059 ± 1.409 μM, respectively (Fig. 4. 7(a)). The percentage of cumulative release at 0.5, 1, 2, 6, 24 and 48 hours were 2.1 ± 1.1%, 2.8 ± 1.2%, 4.3 ± 1.5%, 9.4 ± 1.6%, 15.5 ± 2.5% and 16.6 ± 2.1%, respectively (Fig. 4. 7(b)). The result suggests the effective concentration of FA on oxidative stress induced by 100 μM H_2O_2 may lower than 10 μM.

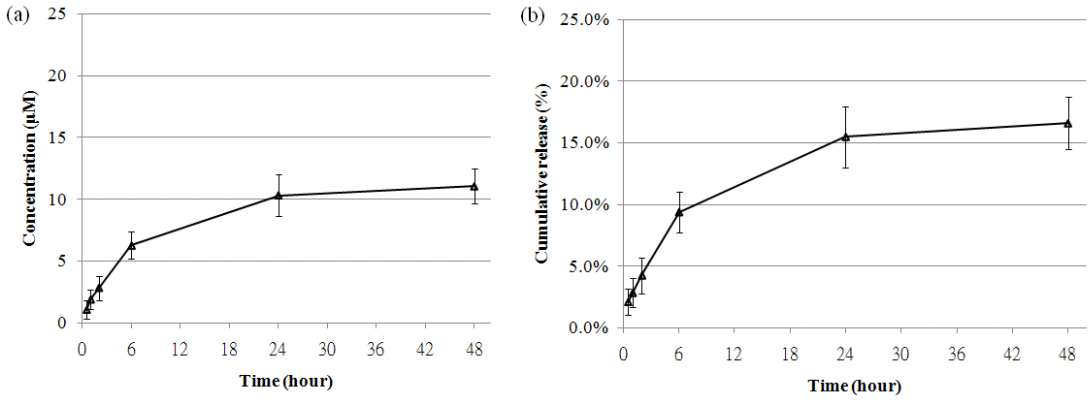

Fig. 4. 7 The release profile of 500 μM FA from C/G/GP hydrogels: (a) the cumulative concentration of FA and (b) cumulative percent release of FA in the PBS at 37 °C.

4.4.2 Gene expression

NP cells induced by 100 μM H_2O_2 for 30 minutes without and with FA in the C/G/GP hydrogel were designed and abbreviated as Gel and Gel-FA group, respectively. The fresh NP cells were the control group and the fold would be normalized to 1 for each gene expression that would be compared with those of in Gel group and Gel-FA group.

Aggrecan, type II collagen and *type I collagen* were the ECM related genes. As shown in Fig. 4. 8, the gene expression of *aggrecan* was significantly down-regulated in Gel group with 0.7833-folds to the control group. There was no significant difference in the expression of *aggrecan* between the control group and Gel-FA group. There was no significant difference between the control group and Gel group in the expression of *type II collagen*. The expression of *type II collagen* was significantly up-regulated in Gel-FA group (1.3689 ± 0.1732) compared with Gel group (1.0827 ± 0.3000). There was no significant difference in *type I collagen* expression between experimental groups (Gel and Gel-FA) and control groups.

MMP-3 and *TIMP-1* were catabolic gene and anti-catabolic gene, respectively. As shown in Fig. 4. 8, the expression of *MMP-3* was 1.4057-folds higher than that of control group. There was no significant difference in the expression of *MMP-3* between

the control group and Gel-FA group. The expression of *MMP-3* was significantly down-regulated in Gel-FA group (0.9911 ± 0.0736) compared with Gel group (1.4057 ± 0.2177). *TIMP-1* was significantly down-regulated in Gel group and Gel-FA group with 0.4319-folds and 0.3832-folds, respectively, to the control group. There was no significant difference in *TIMP-1* expression between Gel group (0.4319 ± 0.0826) and Gel-FA (0.3832 ± 0.1308) group.

TGF-β, BMP-7 and *IGF-1*were the anabolic related genes. As shown in Fig. 4. 8, the expression of *TGF-β* was significantly up-regulated in Gel group with1.3853-folds to control group. There was no significant difference in *TGF-β* expression between Gel-FA group and control group. The expression of *TGF-β* in Gel group (1.3853 ± 0.1464) was higher than that of in Gel-FA group (1.0539 ± 0.0485). There was no significant difference in *BMP-7* expression between experimental groups (Gel and Gel-FA) and control groups. The expression of *IGF-1* was no significant difference for all the groups.

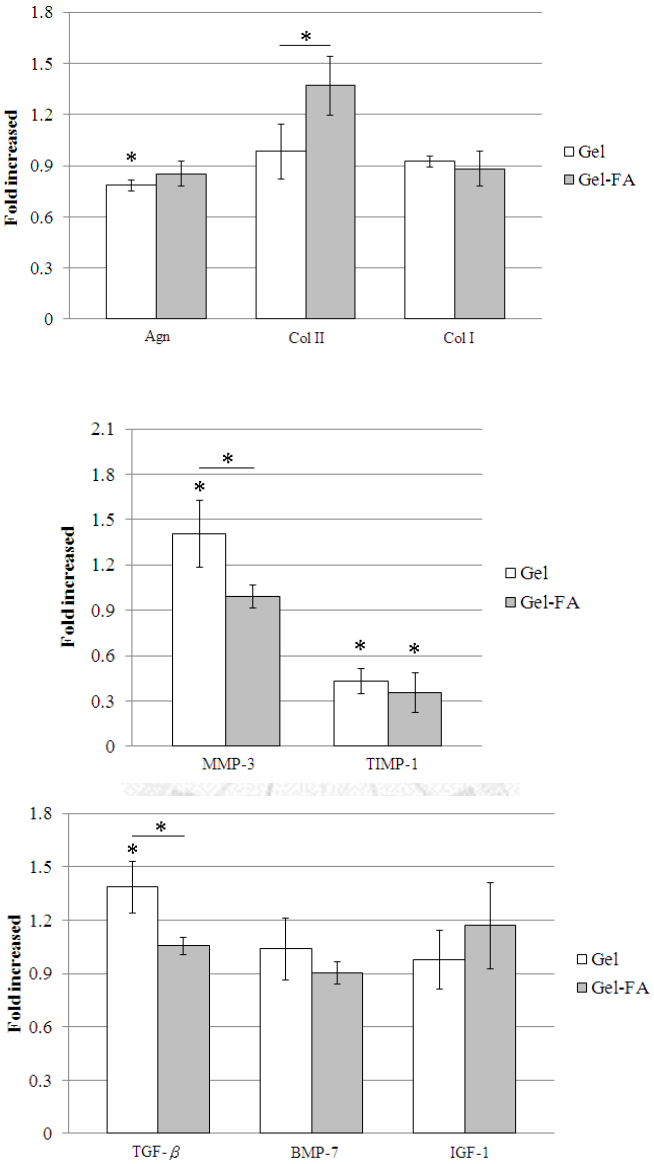

Fig. 4. 8 Gene expression of normal NP cells (without treatment), post-treatment of C/G/GP hydrogel on 100 μM H_2O_2-induced oxidative stress NP cells (Gel) and post-treatment of FA-incorporated C/G/GP hydrogel on 100 μM H_2O_2-induced oxidative stress NP cells (Gel-FA). The result was expressed as fold increase compared with normal NP cells. Each target gene was normalized to GAPDH (n = 3, *, $p < 0.05$).

4.4.3 Sulfated glycosaminoglycan production

The sulfated GAGs production was analyzed by DMMB binding method and normalized to cell numbers by total DNA assay (sulfated GAGs to DNA ratio). As shown in Fig. 4. 9, the sulfated GAGs to DNA ratio in Gel group (0.754 ± 0.051) was significantly lower than that in control group (1 ± 0.070). There was no significant difference in the ratio between the Gel-FA group (0.883 ± 0.109) and control group (1 ± 0.070).

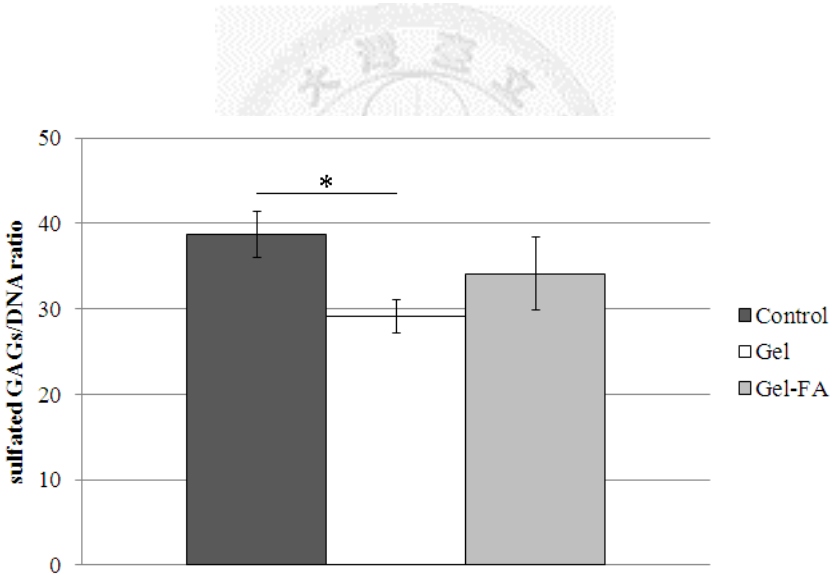

Fig. 4. 9 The ratio of sulfated GAGs to DNA of normal NP cells (without treatment, Control), post-treatment of C/G/GP hydrogel on 100 μM H_2O_2-induced oxidative stress NP cells (Gel) and post-treatment of FA-incorporated C/G/GP hydrogel on 100 μM H_2O_2 induced oxidative stress NP cells (Gel-FA) (n = 3,*, $p < 0.05$).

4.4.4 Alcian blue staining

The samples were stained with alcian blue and kernechtrot (nuclear fast red) at the end of 1-day culture. The alcian blue staining was positive in the control group and Gel-FA group as shown in Fig. 4. 10(a) and Fig. 4. 10(c), respectively. Gel group (Fig. 4. 10(b)), on the contrary, showed relatively light blue color. The results showed that the Gel group and control group had a higher production in sulfated GAGs in the ECM.

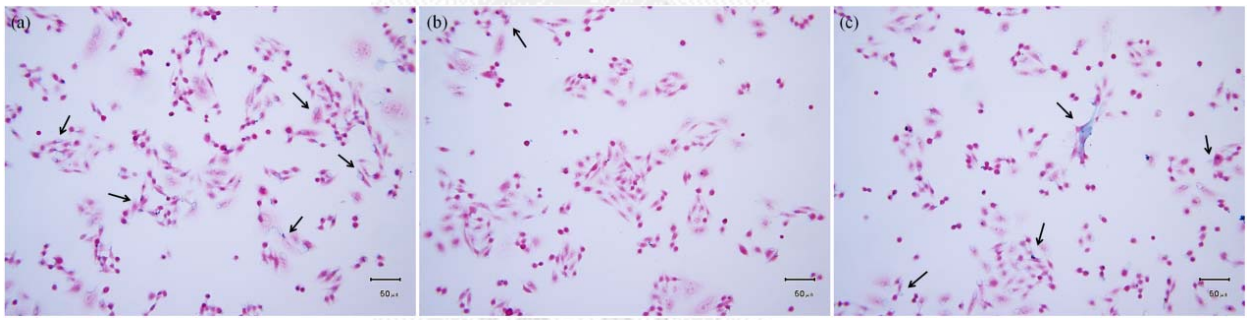

Fig. 4. 10 Alcian blue and nuclear fast red staining of (a) normal NP cells (without treatment, Control), (b) post-treatment of C/G/GP hydrogel on 100 μM H_2O_2-induced oxidative stress NP cells (Gel) and (c) post-treatment of FA-incorporated C/G/GP hydrogel on 100 μM H_2O_2 induced oxidative stress NP cells (Gel-FA). Sulfated GAGs (arrow) were observed at the end of 1-day culture.

4.4.5 Caspase-3 activity

The activity of caspase-3 was strongly associated with apoptosis. As shown in Fig. 4. 11, the caspase-3 activity of Gel group was 1.259 ± 0.030 that was much higher ($p < 0.05$) than that of control group (1 ± 0.045). There was no significant difference in caspase-3 activity between Gel-FA group (1.079 ± 0.021) and control group (1 ± 0.045). The caspase-3 activity in Gel-FA group (1.079 ± 0.021) was significantly lower than that in Gel group (1.259 ± 0.030).

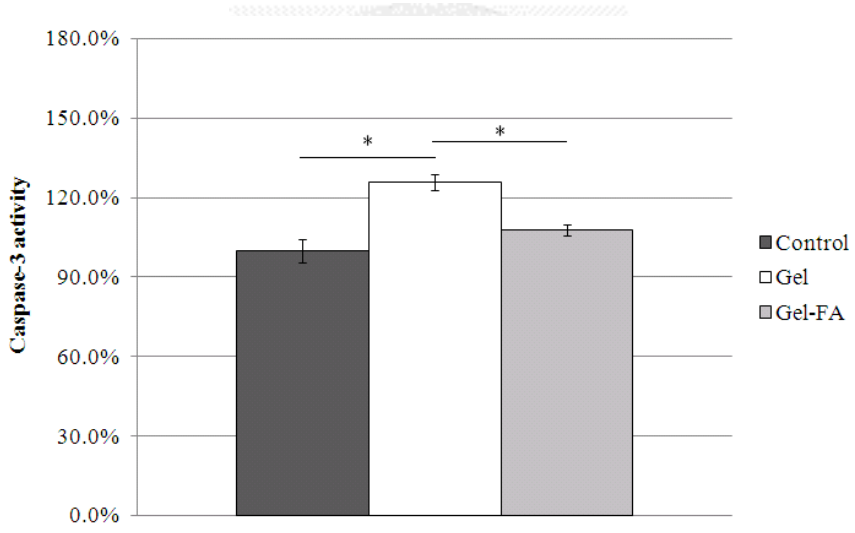

Fig. 4. 11 The caspase-3 activity of normal NP cells (without treatment, Control), post-treatment of C/G/GP hydrogel on 100 μM H_2O_2-induced oxidative stress NP cells (Gel) and post-treatment of FA-incorporated C/G/GP hydrogel on 100 μM H_2O_2 induced oxidative stress NP cells (Gel-FA) (n = 3,*, $p < 0.05$).

4.4.6 TUNEL staining

DNA fragmentation of the NP cells was detected by TUNEL assay which can specifically bind 3'-OH ends of nucleic acids in apoptotic cells. Fig. 4. 12 showed the results of TUNEL staining of control group (Fig. 4. 12(a)), Gel (Fig. 4. 12(b)) and Gel-FA (Fig. 4. 12(c)). As shown in Fig. 4. 12(b), Gel group showed lots of TUNEL-positive (green florescent dye) cells under the examination of confocal microscope. Whereas, there were significantly less TUNEL-positive cells in both control group and Gel-FA group.

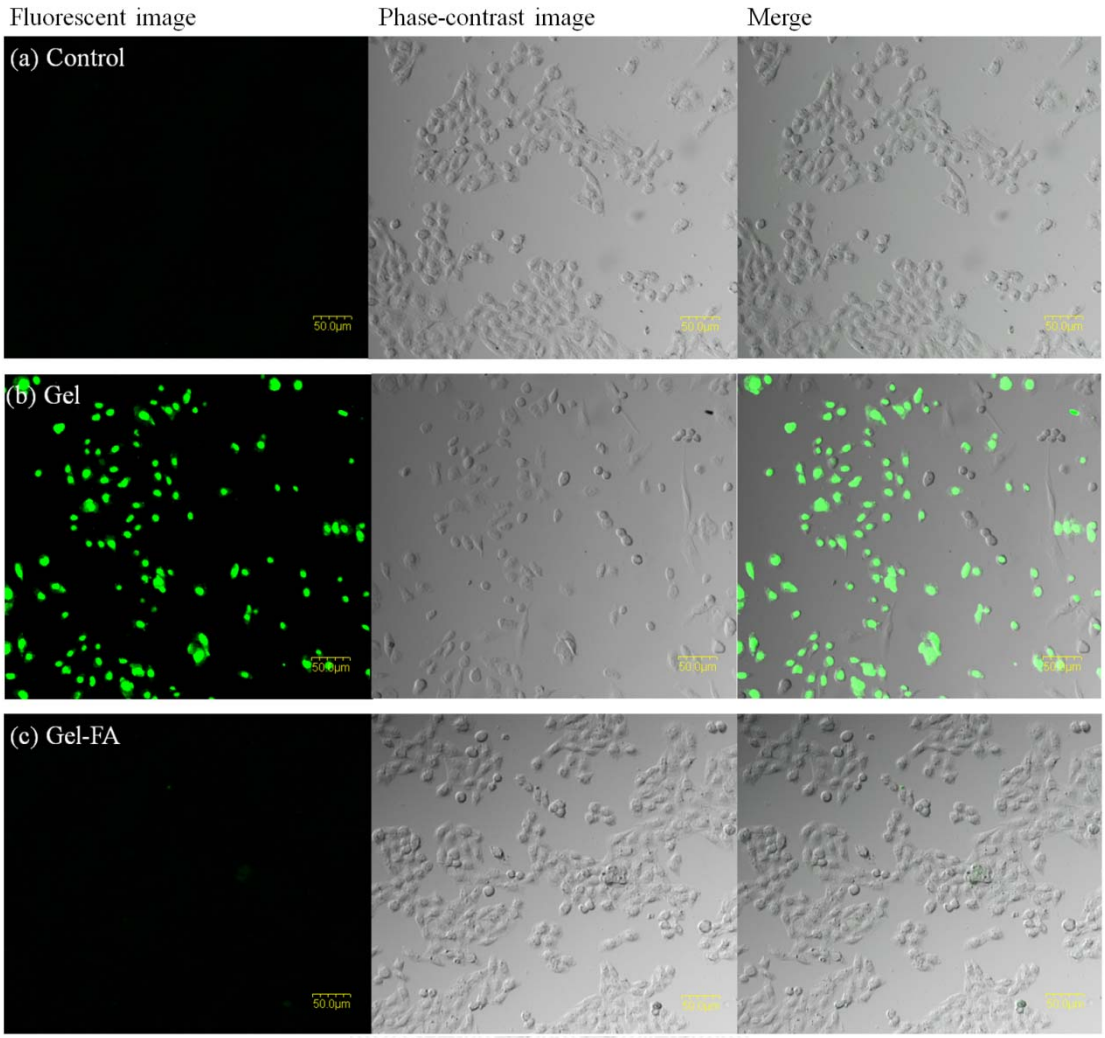

Fig. 4. 12 TUNEL staining of (a) Normal NP cells (without treatment, Control), (b) post-treatment of C/G/GP hydrogel on 100 μM H_2O_2-induced oxidative stress NP cells (Gel) and (c) post-treatment of FA-incorporated C/G/GP hydrogel on 100 μM H_2O_2 induced oxidative stress NP cells (Gel-FA).

4.5 The effects of thermosensitive ferulic acid-immobilized chitosan/gelatin/β-glycerol phosphate (FA-immobilized C/G/GP) hydrogel on nucleus pulposus cells under hydrogen peroxide-induced oxidative stress

4.5.1 TNBS assay

Residual amino group of FA-immobilized gelatin were evaluated by TNBS assay. TNBS reacts with amino groups of gelatin to form the TNBS-amino acid complex products. The residual amino group of gelatin (without immobilization of FA) was designed as 100% than compared with FA-immobilized gelatin group. After immobilization of FA on the gelatin, the residual amino group of gelatin was significantly decreased 61.9% compared with gelatin group (without immobilization of FA) as shown in Fig. 4. 13.

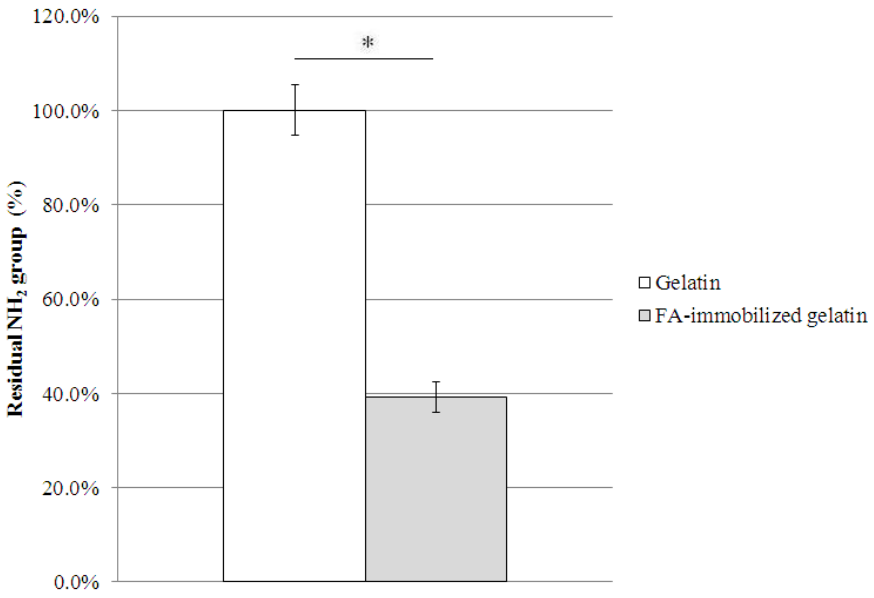

Fig. 4. 13 The percentage of residual amino groups in the gelatin (without immobilization of FA) and FA-immobilized gelatin group. The gelatin group was designed as 100% than compared with FA-immobilized gelatin group (n = 3,*, $p < 0.05$).

4.5.2 Reheological characterization

Gelation temperature and gelation time of the FA-immobilized C/G/GP solution were determined at which elastic modulus (G') is equal to viscous modulus (G''). As shown in Fig. 4. 14(a), the gelation temperature of FA-immobilized C/G/GP solution was 31.80°C. The gelation time of FA-immobilized C/G/GP solution was 60.81 seconds at 37°C (Fig. 4. 14(b)). The FA-immobilized C/G/GP solution was kept in liquid form even the time was extended to 15 minutes at 25 °C (Fig. 4. 14(c)).

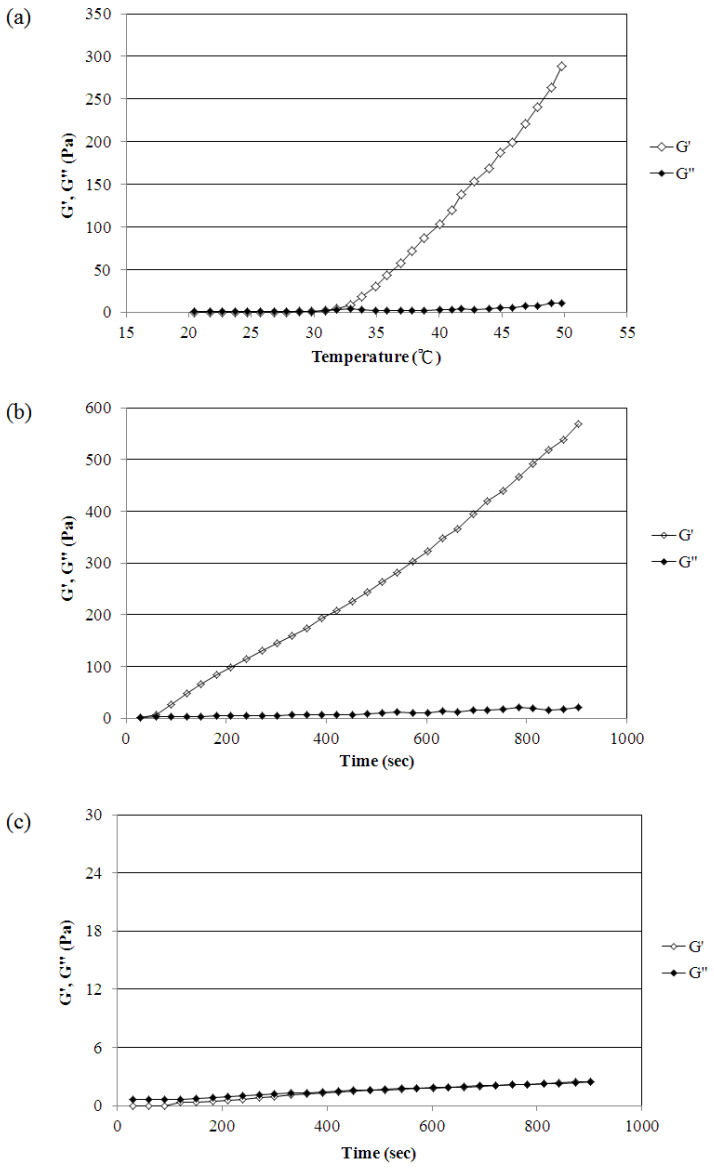

Fig. 4. 14 (a) Temperature dependence of storage modulus (G') and loss modulus (G"), (b) time dependence of G' and G" at 37 °C and (c) time dependence of G' and G" at 25 °C. The gelation time of FA-immobilized C/G/GP solution is 31.80 °C. The gelation time of FA-immobilized C/G/GP solution at 37 °C and 25 °C are 60.81 and over 900 seconds respectively.

4.5.3 Cytotoxicity of thermosensitive FA-immobilized C/G/GP hydrogel on NP cells

NP cells were cultured in the extraction medium obtained from the developed hydrogel. The mitochondrial activity was evaluated by WST-1 assay. As shown in Fig. 4. 15(a), the OD value of the control group on day 1 and day 3 were 1.256 ± 0.069 and 1.467 ± 0.059, respectively. The OD value of the FA-immobilized group on day 1 and day 3 were 1.223 ± 0.033 and 1.493 ± 0.112, respectively. The results of WST-1 showed that there was no significant difference in OD value between the control group and FA-immobilized group on day1 and day 3.

The results of LDH assay was expressed in percentage of cytotoxicity. As shown in Fig. 4. 15(b), the cytotoxicity of control group on day 1 and day 3 were 8.5 ± 0.1% and 10.2 ± 0.9%, respectively. The cytotoxicity of FA-immobilized group on day 1 and day 3 were 7.8 ± 0.9% and 8.6 ± 0.8%, respectively. There was no significant difference in cytotoxicity between control group and FA-immobilized group.

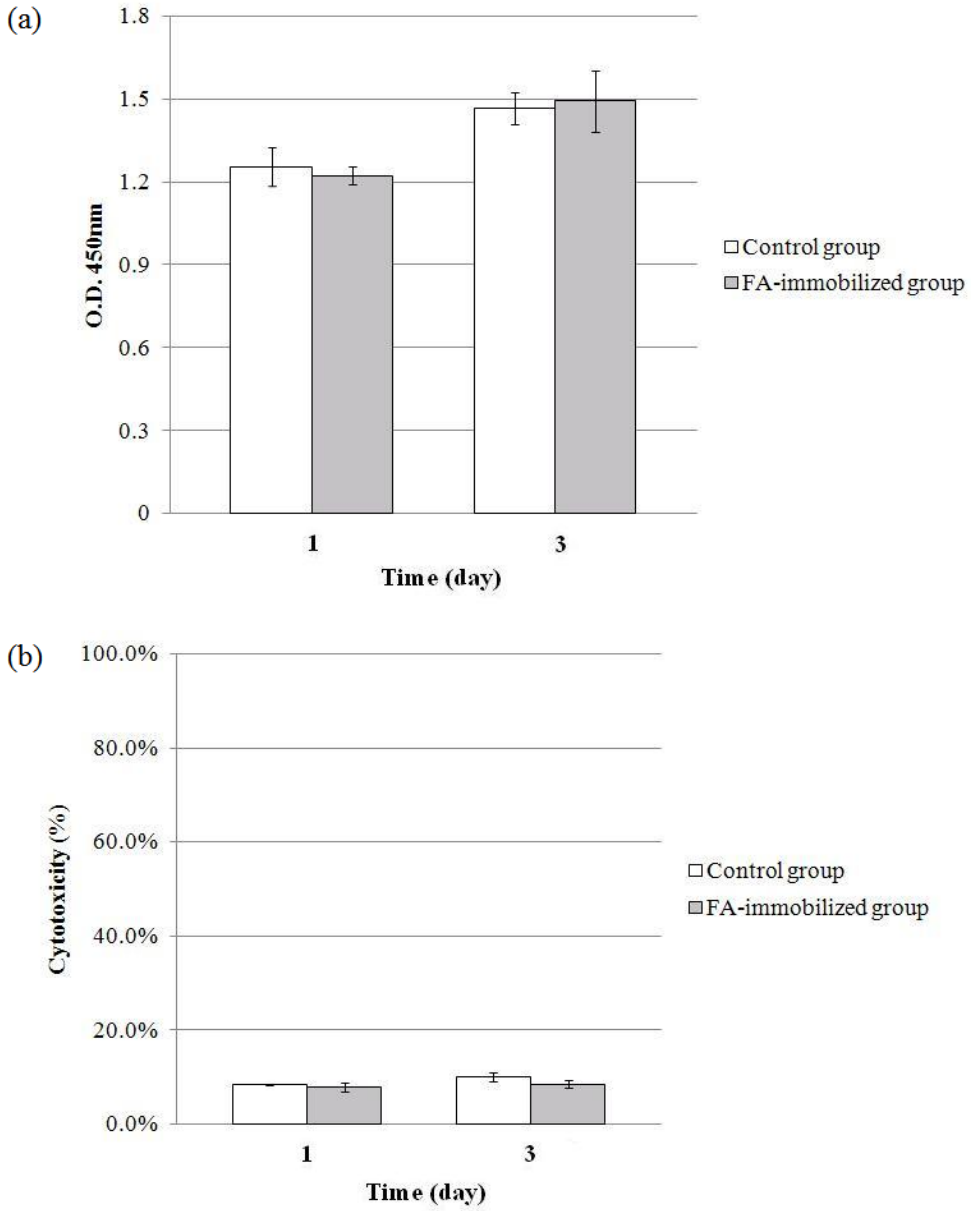

Fig. 4. 15 Cytotoxicity of FA-immobilized C/G/GP to NP cells: (a) WST-1 assay (n = 3, $p > 0.05$) and (b) LDH assay (n = 3, $p > 0.05$).

4.5.4 The release of FA from FA-immobilized C/G/GP hydrogel

Fig. 4. 16 shows the release profile of FA from the FA-immobilized C/G/GP hydrogel. The cumulative concentration of FA in the PBS at 0.5, 1, 2, 6, 24 and 48 hours were 1.167 ± 0.179, 1.064 ± 0.262, 1.251 ± 0.189, 2.097 ± 0.230, 5.166 ± 0.124 and 5.206 ± 0.291 μM, respectively (Fig. 4. 16(a)). The percentage of cumulative release at 0.5, 1, 2, 6, 24 and 48 hours were 1.7 ± 0.6%, 1.8 ± 0.5%, 2.2 ± 0.3%, 3.6 ± 0.4%, 9.5 ± 0.9% and 9.3 ± 0.7%, respectively (Fig. 4. 16(b)).

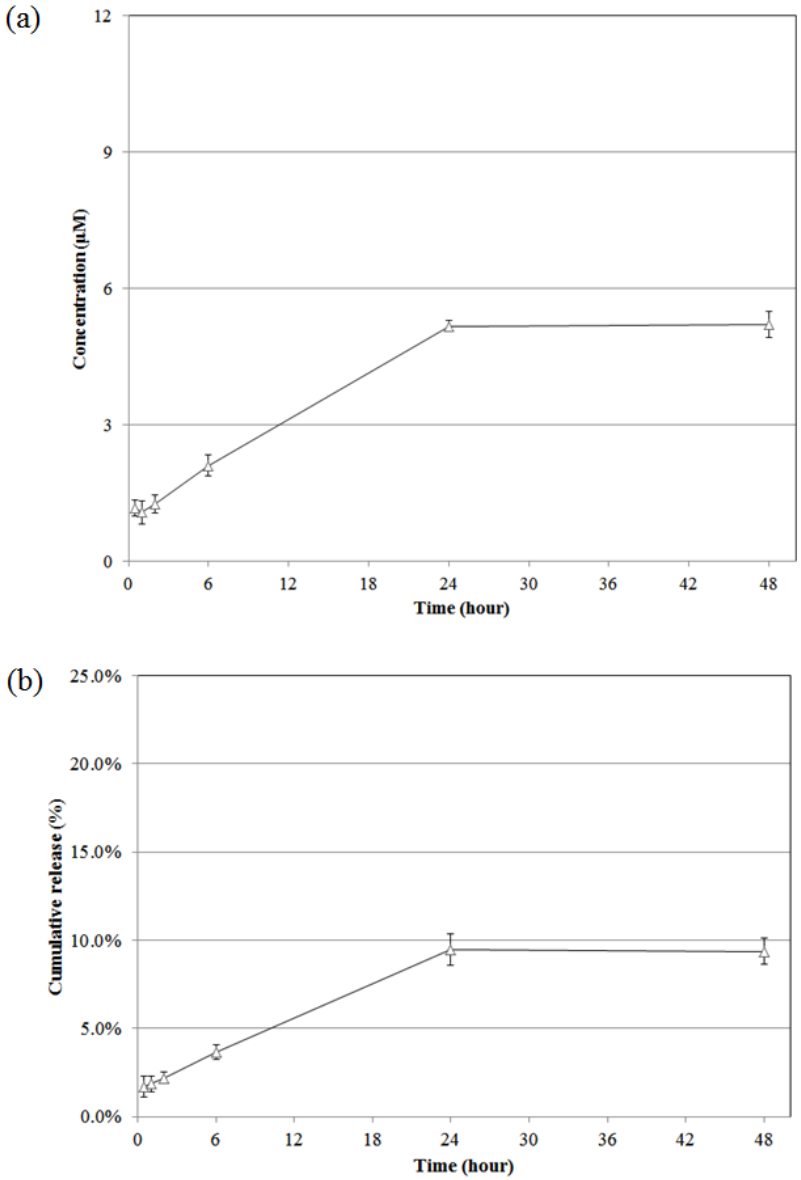

Fig. 4. 16 The release profile of FA from FA-immobilized C/G/GP hydrogel: (a) cumulative percentage and (b) the cumulative concentration of FA in the PBS at 37 °C.

4.5.5 Gene expression

NP cells stimulated with 100 μM H_2O_2 for 30 minutes and then incubated with FA-immobilized C/G/GP hydrogel or C/G/GP hydrogel (without immobilization of FA) for 2 hours were designed and abbreviated as C/G/GP and FA-immobilized C/G/GP group, respectively. The results of mRNA gene expression were reported as fold increase compared with fresh NP cells (control group).

Inducible nitric oxide synthase (*iNOS*) and *interlukin-1β* (*IL-1β*) are pro-inflammatory genes. As shown in Fig. 4. 17, the expression of *iNOS* and *IL-1β* were significantly up-regulated in C/G/GP group with 2.6237 and 1.8636-folds to the control group, respectively. There was no significant difference in the expression of *iNOS* and *IL-1β* between the control group and FA-immobilized C/G/GP group. The expression of *iNOS* was significantly higher in C/G/GP group (2.6237 ± 0.3886) compared with FA-immobilized C/G/GP group (1.0987 ± 0.0989). The expression of *IL-1β* was significantly up-regulated in C/G/GP group (1.836 ± 0.1295) compared with FA-immobilized C/G/GP group (1.2175 ± 0.1664). *Type II collagen* (*Col II*)*, aggrecan* (*Agn*) and *type I collagen* (*Col I*) are the ECM component genes. As shown in Fig. 4. 17, the expression of *type II collagen* and *aggrecan* were significantly down-regulated in C/G/GP group with 0.7856 and 0.6737-folds to the control group, respectively. The

expression of *type II collagen* was significantly higher in FA-immobilized C/G/GP group (1.1600 ± 0.0477) compared with other groups. There was no significant difference in the expression of *aggrecan* between the control group and FA-immobilized C/G/GP group. The expression of *type I collagen* was significantly lower in FA-immobilized C/G/GP group (0.7214 ± 0.1977) compared with C/G/GP group (1.2029 ± 0.1301). There was no significant difference in the expression of *type I collagen* between the control group and experimental group (C/G/GP group and FA-immobilized C/G/GP group). *Matrix metalloproteinase-3* (*MMP-3*) and *tissue inhibitor of metalloproteinase-1* (*TIMP-1*) are catabolic gene and anti-catabolic gene respectively. As shown in Fig. 4. 17, the expression of *MMP-3* and *TIMP-1* were significantly up-regulated in C/G/GP group with 3.3934 and 1.4314-folds to the control group, respectively. There was no significant difference in the expression of *MMP-3* and *TIMP-1* between the control group and FA-immobilized C/G/GP group. The expression of *MMP-3* and *TIMP-1* were significantly down-regulated in FA-immobilized C/G/GP group compared with C/G/GP group. *Transforming growth factor-β* (*TGF-β*), *bone morphogenic protein-7* (*BMP-7*) and *insulin-like growth factor-1* (*IGF-1*) are anabolic related genes. As shown in Fig. 4. 17, the expression of *TGF-β* was significantly higher in C/G/GP group (1.6735 ± 0.3179) compared with control group. There was no significant difference in the expression of *TGF-β* between the control group and

FA-immobilized C/G/GP group. Fig. 4. 17 showed that there was no significant difference in the expression of *BMP-7*and *IGF-1* between experimental group and control group.

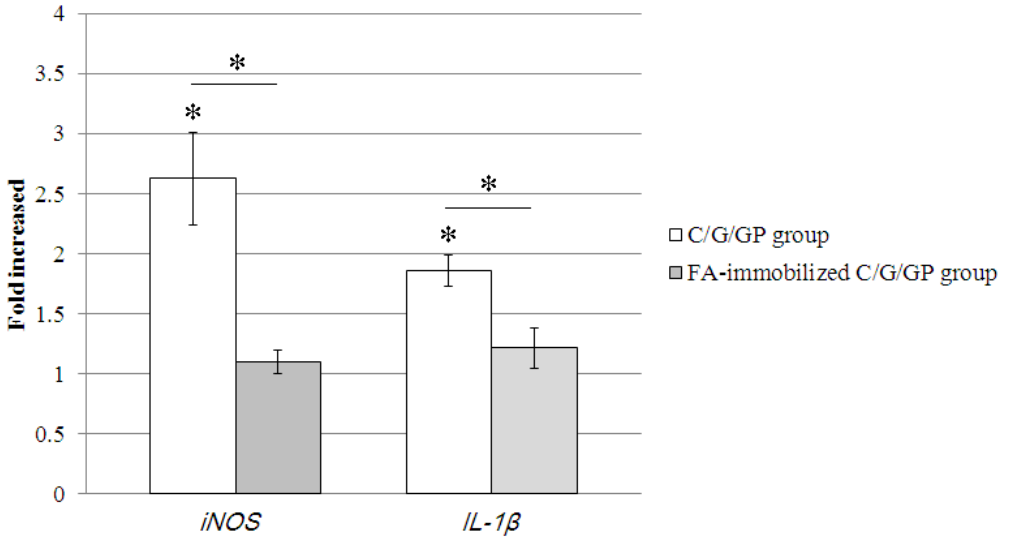
Fold increased
4
3.5
3
2.5
2
1.5
1
0.5
0
iNOS
IL-1β
C/G/GP group
FA-immobilized C/G/GP group

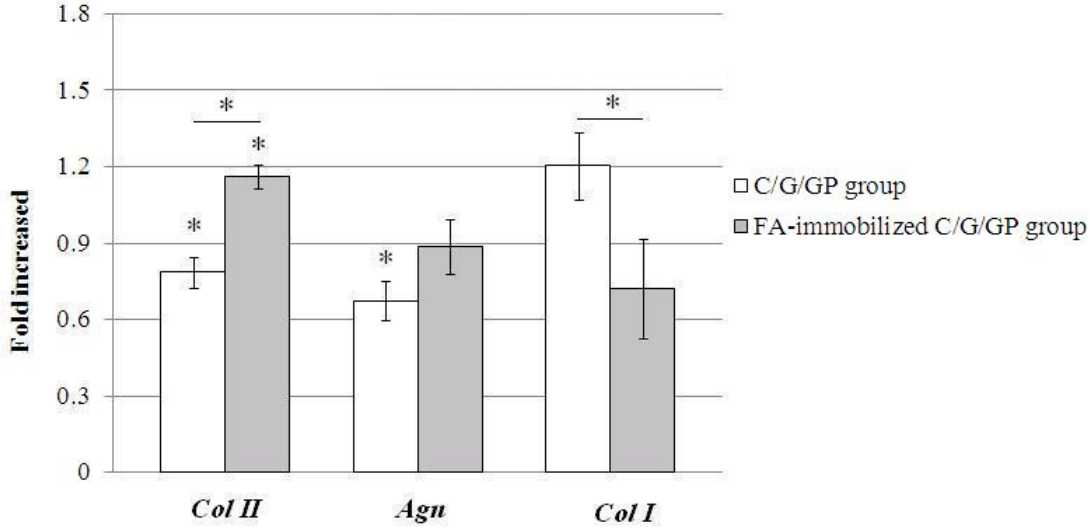
Fold increased
1.8
1.5
1.2
0.9
0.6
0.3
0
Col II
Agn
Col I
C/G/GP group
FA-immobilized C/G/GP group

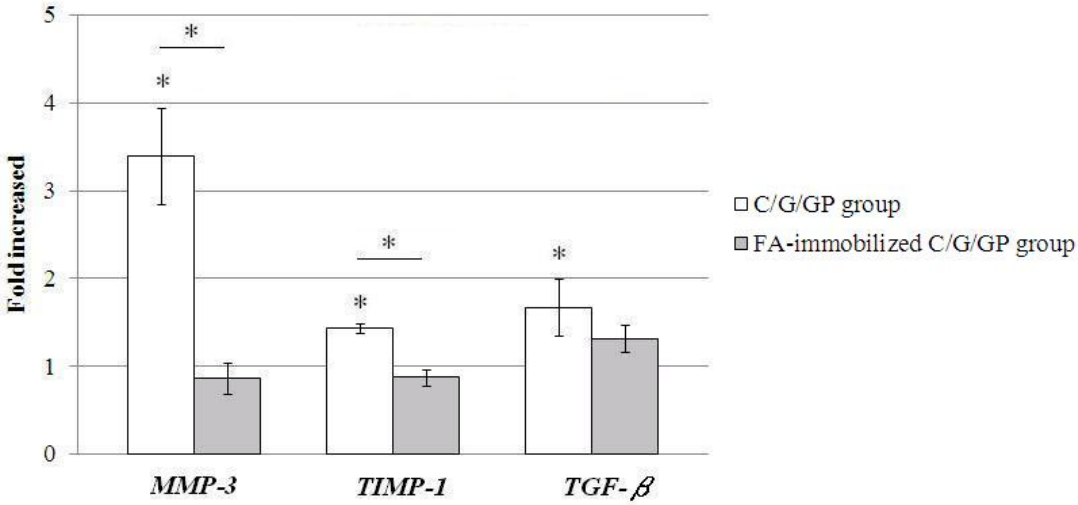
Fold increased
5
4
3
2
1
0
MMP-3
TIMP-1
TGF-β
C/G/GP group
FA-immobilized C/G/GP group

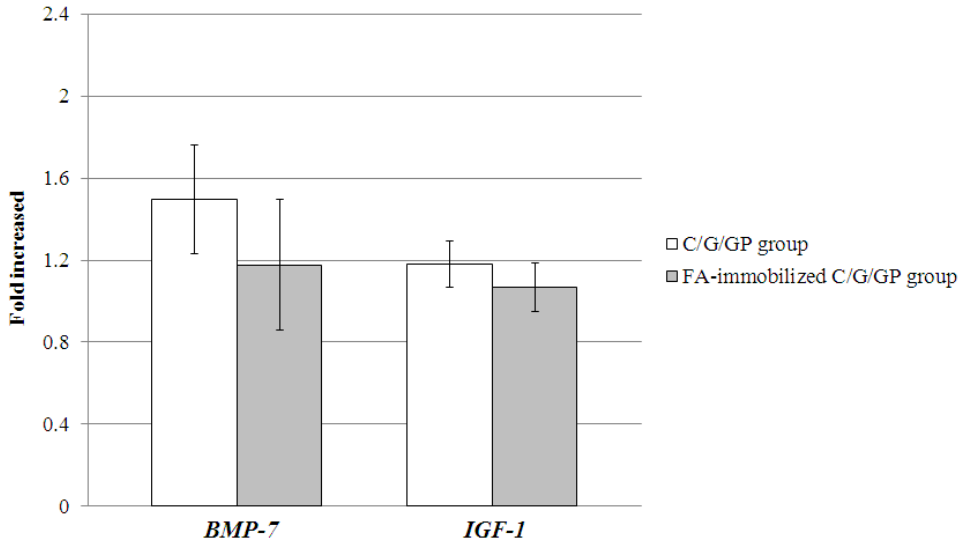

Fig. 4. 17 Gene expression of the normal NP cells (without treatment, control group), post-treatment of C/G/GP hydrogel on 100 μM H_2O_2-induced oxidative stress NP cells (C/G/GP group) and post-treatment of FA-immobilized C/G/GP hydrogel on 100 μM H_2O_2 induced oxidative stress NP cells (FA-immobilized C/G/GP group). The result was expressed as fold increase compared with normal NP cells. Each target gene was normalized to GAPDH (n = 3, *, $p < 0.05$).

4.5.6 Sulfated glycosamninoglycan production

The results of sulfated GAG production were normalized to cell number. As shown in Fig. 4. 18, the sulfated GAG production per cell was significantly decreased in C/G/GP group (0.775 ± 0.105) compared with other groups. There was no significant difference in the sulfated GAG production between the control group (1.228 ± 0.196) and the FA-immobilized C/G/GP group (1.389 ± 0.082).

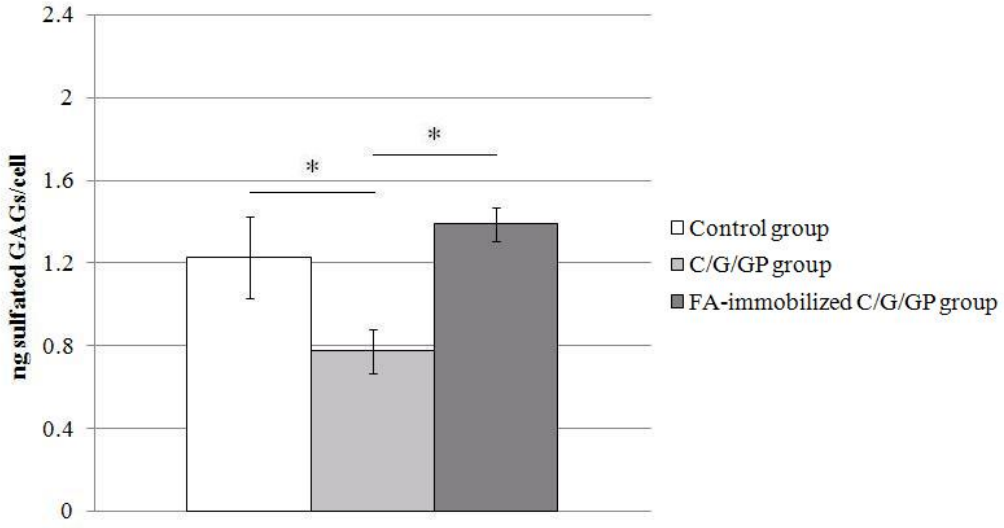

Fig. 4. 18 The sulfated GAGs production per cell in normal NP cells (without treatment, control group), post-treatment of C/G/GP hydrogel on 100 μM H_2O_2-induced oxidative stress NP cells (C/G/GP group) and post-treatment of FA-immobilized C/G/GP hydrogel on 100 μM H_2O_2 induced oxidative stress NP cells (FA-immobilized C/G/GP group) (n = 3,*, $p < 0.05$).

4.5.7 Caspase-3 activity

Activation of caspase-3 was highly associated with apoptosis. The results of caspase-3 activity were expressed in percentage. As shown in Fig. 4. 19, the caspase-3 activity was significantly increased in C/G/GP group (126.5 ± 5.5%) compared with control group (97.7 ± 1.0%). There was no significant difference in caspase-3 activity between FA-immobilized C/G/GP group (96.1 ± 4.8%) and control group.

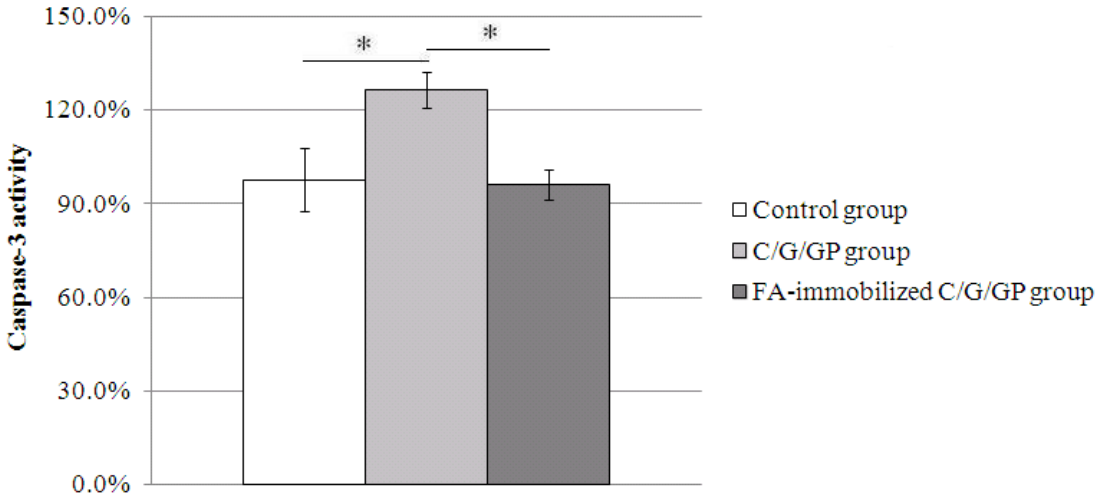

Fig. 4. 19 The caspase-3 activity in normal NP cells (without treatment, control group), post-treatment of C/G/GP hydrogel on 100 μM H_2O_2-induced oxidative stress NP cells (C/G/GP group) and post-treatment of FA-immobilized C/G/GP hydrogel on 100 μM H_2O_2 induced oxidative stress NP cells (FA-immobilized C/G/GP group) (n = 3,*, $p <$ 0.05).

4.5.8 TUNEL staining

Detection of apoptosis was performed by TUNEL assay which can label the nuclei of apoptotic cells. There were lots of TUNEL-positive cells in C/G/GP group (Fig. 4. 20(b)). In contrast, there were significantly less TUNEL-positive cells in both control group (Fig. 4. 20(a)) and FA-immobilized C/G/GP group (Fig. 4. 20(c)).

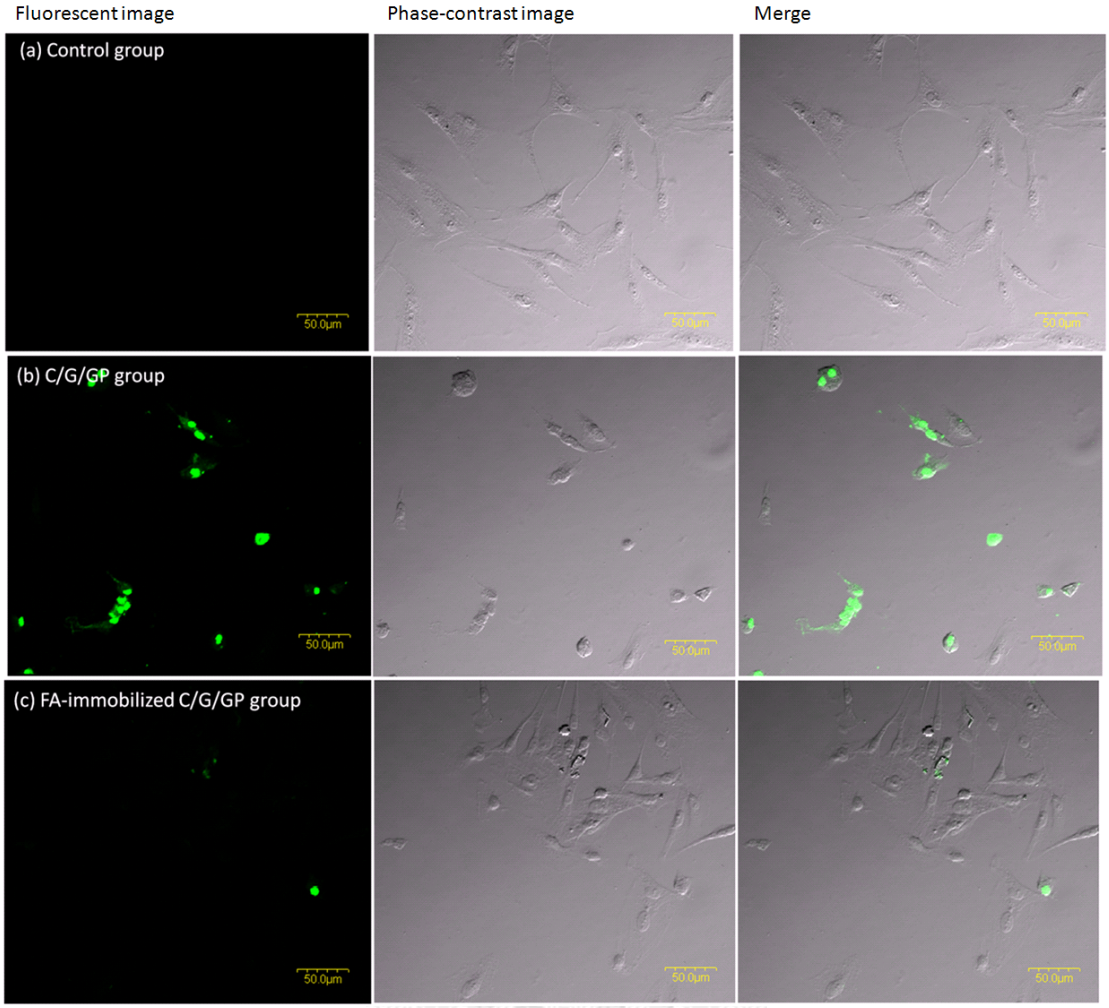

Fig. 4. 20 TUNEL staining of (a) Normal NP cells (without treatment, control group), (b) post-treatment of C/G/GP hydrogel on 100 μM H_2O_2-induced oxidative stress NP cells (C/G/GP group) and (c) post-treatment of FA-immobilized C/G/GP hydrogel on 100 μM H_2O_2 induced oxidative stress NP cells (FA-immobilized C/G/GP group).

CHAPTER 5 DISCUSSIONS

WST-1 assay was commonly used to determine the mitochondrial activity; and crystal violet assay was used to evaluate the cell number. As shown in Fig. 4. 1, the OD value of WST-1 and crystal violet assay was both increased in FA500 group. We could tell that the increase of mitochondrial activity was due to the increase of cell number. The antioxidant such as vitamin C, vitamin E and uric acid have been reported those could improve cell adhesion and proliferation [65-67]. From the results of crystal violet assay and WST-1 assay, we believe that cell number increasing in the FA-treated group might be partly due to anti-apoptosis. As the result of LDH assay (Fig. 4. 1), it showed a very high cytotoxicity in FA5000 group. On the contrary, there was no significant cytotoxicity to NP cells if FA was lower than 500 μM (FA500 group). Commonly, overproduction of ROS, but below set point, could be regulated by several antioxidants including glutathione, vitamin A, vitamin C and vitamin E. However, antioxidants may become insufficient if exogenous ROS overflow in, which may lose homeostasis to impair cell functions [68]. FA is one of potent free radical scavenger, which can terminate the series of ROS reactions. In the high concentration of FA, it may interrupt the cell proliferation due to ROS below the set point that may result in cell death. From the study of LDH assay, we believe the optimum FA would be approximately in 500

μM. If FA level is higher than the optimum, it might lead ROS below set point and interrupt the cell proliferation.

5.1 The effects of ferulic acid on hydrogen peroxide-induced oxidative stress nucleus pulposus cells

Kim et al. [34] reported that the H_2O_2 content was 0.13 ± 0.09 μmole in the grade II degeneration of human NP. Wei et al. [41] showed that apoptosis of NP cells could be induced by 100 μM of H_2O_2. Therefore, the 100 μM of H_2O_2 was be used to induce the oxidative stress in the study. Fig. 4. 2 showed the oxidative stress induced by 100 μM H_2O_2 can be significantly decreased to normal level by 0.5 μM of FA (H100FA0.5 group).

In the degenerated NP, type II collagen and proteoglycans would both be down regulated; whereas type I collagen was up-regulated; however, the changes of collagen are not as significant as those of proteoglycans [2]. Lower molecular weight of type II collagen or GAGs would be sporadically observed in the extracellular matrix. As shown in Fig. 4. 3, the mRNA gene expression of *aggrecan* was down regulated in H100 group. The expression of *aggrecan* and *type II collagen* were significantly up regulated in H100FA500 group. We believe that FA might promote desired ECM synthesis. Matrix metalloproteinases (MMPs) have been found over secretion in degenerated NP extracelular matrix. As known, MMP-3 is one of major enzymes to degrade type II collagen and aggrecan in ECM [29]. As shown in Fig. 4. 3, *MMP-3* expression in

H100FA500 group was much lower than that in H100 group. *TIMP-1* was higher expression in H100FA500 group than that in H100 group (Fig. 4. 3) that might be in response to the *MMP-3* expression. ROS have been reported that can promote MMPs synthesis by up-regulation of cytokines such as tumor necrosis factor-α (TNF-α), interleukin-1 (IL-1) and inducible nitric oxide synthase (iNOS) [4]. Recent studies revealed that antioxidants could down-regulate the expression of pro-inflammatory genes such as IL-1, iNOS and TNF-α [45, 69]. Moreover, the positive induction of TIMPs can be stimulated by antioxidants such as vitamin A analogs, which can inhibit the MMPs activity [29]. From the results, we believe that FA may have the ability to inhibit the activity of *MMP-3* and promote *TIMP-1* synthesis (Fig. 4. 3). Anabolic factors such as TGF-β, BMP-7 and IGF-1 were generally to promote the synthesis of extracellular matrix [9, 21]. In the study (Fig. 4. 3), the *TGF-β* expression in H100 group was much higher than that of H100FA500 group that sounded against the previous results. However, TGF-β has been reported that highly expressed in the matrix of degenerated disc [22-24]. They believed that might be due to negative feedback control in the attempt of the degenerative disc cells to replenish the degraded ECM. By the way, the expression of *TGF-β* was no significant difference to the control group (Fig. 4. 3). We may say that the FA might switch *TGF-β* expression back to normal in H_2O_2-damaged NP cells. BMP-7 can stimulate the synthesis of type II collagen and

proteoglycans in NP cells; and shows the dose-dependent effects in the expression of aggrecan and type II collagen [9, 21]. As shown in Fig. 4. 3, the expression of *BMP-7* was up regulated in H100FA500 group. We could expect that the up-regulation of *BMP-7* is associated with increased expression of *aggrecan* and *type II collagen* as shown in Fig. 4. 3.

In the degenerated NP, a decrease in chondroitin sulfate has been reported, which results in a decrease in water content of NP and a decrease in capability of NP to response the external stress [70-71]. ROS have been observed in degenerated NP, which could directly damage the cell and cause to ECM degradation [72-74]. Fig. 4. 4 showed the sulfated GAGs to DNA ratio of H_2O_2-induced oxidative stress NP cells (H100 group) was significantly lower than that of in normal NP cells (control group). After FA treated (H100FA500 group), ratio turned up and back to the normal condition. The results indicated that post-treatment of FA on H_2O_2-induced oxidative stress NP cells might restore the cell function to produce appropriate ECM.

Apoptosis can be initiated *via* extrinsic or intrinsic pathway which depends on apoptotic stimuli [37]. The ROS-mediated apoptosis is through the intrinsic pathway, which results in the release of cytochrome c from mitochondria. The complex of cytochrome c-Apaf-1 (apoptotic protease activating factor-1) activates the procaspase-9

which leads to activation of caspase-3 [37-39]. As shown in Fig. 4. 5, the caspase-3 activity was significantly increased in H100 group. The caspase-3 activity was decreased to normal level when post-treatment of FA on H_2O_2-induced oxidative stress NP cells (H100FA500 group). Nuclear condensation and segmentation can be observed in apoptotic cells. The number of DNA 3'-OH are associated with DNA fragmentation which caused by apoptosis [40]. The results of TUNEL stain showed that only few apoptotic nuclei was in H100FA500 group but compared with H100 group as shown in (Fig. 4. 6). Kim et al. [36] suggested that caspase inhibitors can effectively inhibit the oxidative stress-induced apoptosis of disc cells. Wei et al. [41] reported that BMP-7 can prevent the apoptosis of NP cells by inactivation of caspase-3. In our study, the results indicate that FA can inhibit the capase-3 activity and then prevent the NP cells from the damage caused by ROS. Therefore, FA may repair the degenerative NP, which may be a potent therapeutic molecule for early IVD degeneration.

5.2 Thermosensitive chitosan/gelatin/β-glycerol phosphate hydrogel as a controlled release system of ferulic acid for nucleus pulposus regeneration

The release profile of FA from C/G/GP hydrogel was shown in Fig. 4. 7. The C/G/GP hydrogel released ~2% of FA in the first 0.5 hours, and the cumulative concentration of FA in the PBS was 1.058 ± 0.740 μM. As shown in Fig. 4. 2, this cumulative concentration of FA in the first 0.5 hours was enough to terminate the free radical reaction induced by 100 μM H_2O_2. Ruel-Gariépy et al. [62] reported that almost 80% of hydrophilic compounds incorporated in the thermosensitive C/GP hydrogel were released in the first 24 hours. On the contrary, C/GP hydrogel containing hydrophobic compounds can sustain the delivery for at least 1 month [63]. In our study, the C/G/GP hydrogel showed sustained slow release of FA after 24 hours (Fig. 4. 7). The results showed that C/G/GP hydrogel have the potential to be used as sustained-release system for hydrophobic compounds such as FA.

In the degenerated NP, loss of proteoglycans, decrease in type II collagen and increase in type I collagen were observed, however, the changes of collagen are not as significant as those of proteoglycans [1]. Aggrecan is the major component of the proteoglycans, which play an important role to resist external compressive loads. As shown in Fig. 4. 8, the mRNA gene expression of *aggrecan* was down-regulated in Gel

group compared with control group. There was no significant difference in the expression of *aggrecan* between the control group and Gel-FA group. Overproduction of ROS can influence several cellular signaling pathways including apoptosis, differentiation and inflammation [45]. The pro-inflammatory mediators such as interlukin-1 (IL-1) and tumor necrosis factor-α (TNF-α) inhibit the synthesis of the desired matrix and promote the MMPs production [4]. FA is a phenolic compound and is known to down-regulate pro-inflammatory gene expression, which may inhibit the proteoglycans degradation [45]. Fig. 4. 8 showed that there was no significant difference between the control group and Gel group in the expression of *type II collagen*. The expression of *type II collagen* was significantly up-regulated in Gel-FA group compared with Gel group. Li et al. [75] reported resveratrol, an antioxidant, can prevent proteoglycans degradation. In our study, we propose that FA might treat H_2O_2-induced oxidative stress NP cells to normal status by up-regulation *Aggrecan*; moreover, FA might promote desired ECM synthesis (*type II collagen*).

High level of MMPs have been found in degenerated NP, which can degrade the proteoglycans and type II collagen of the ECM [2]. It has been reported that overproduction of ROS can up-regulate the MMPs activity by intracellular signaling pathways [4]. As shown in Fig. 4. 8, the expression of *MMP-3* was highly expressed in

Gel group, and then express in normal level in Gel-FA group. As known, FA is a free radical scavenger that may contribute to the anti-inflammatory effect by down-regulation of *MMP-3*.

TGF-β, BMP-7 and IGF-1 are known as anabolic factors which can promote the synthesis of proteoglycans and type II collagen [21, 69]. However, recent studies demonstrated that the up-regulation of *TGF-β* might relate to inflammatory reaction in the degenerated NP [9, 22]. The strong expression of *TGF-β* reflects that the disc cells attempt to repair the degraded ECM. In addition, it has been shown that ROS can stimulate the expression of *TGF-β* in different types of cells [23, 25-26]. Liu et al. [28] reported that ROS induced the expression of *TGF-β via* activation of *MMPs*. As shown in Fig. 4. 8, the expression of *TGF-β* was up-regulated in Gel group, and then down-regulated to normal level in Gel-FA group. We could expect the increase of *TGF-β* with an associated increase in the expression of *MMP-3* as shown in Fig. 4. 8.

In the normal NP, proteoglycans and type II collagen play a role to provide the mechanical support to the disc. Proteoglycans consist of core protein with attached GAGs such as chondroitin sulfate and keratin sulfate. In the degenerated NP, a decrease in the content of chondroitin sulfate results in a decrease of water content that affects the capability of NP to absorb the external stress [1]. Overproduction of ROS can

directly damage the cell and degrade the ECM [71-73]. Fig. 4. 9 showed the sulfated GAGs to DNA ratio of Gel group is significantly lower than normal NP cells (control group). The release of FA from C/G/GP hydrogel can terminate the free radical reaction, and then prevent NP cells from the further damage caused by ROS. As shown in Fig. 4. 9, the sulfated GAGs to DNA ratio was reached to the normal level in the Gel-FA group. The results of alcian blue staining also showed that Gel-FA group was stained positive in sulfated GAGs (Fig. 4. 10(c)). The results indicated that the release of FA from C/G/GP hydrogel might treat H_2O_2-induced oxidative stress NP cells to produce desired ECM.

Apoptosis *via* intrinsic pathway can be initiated by oxidative stress which stimulates cytochrome c release from mitochondria. The formation of cytochrome c-Apaf-1 (apoptotic protease activating factor-1) complex can activate the procaspase-9 that results in the activation of caspase-3. Activation of caspase-3 is strongly associated with apoptosis [37-38, 74]. As shown in Fig. 4. 11, the caspase-3 activity was significantly increased in Gel group compared with control group. The caspase-3 activity was decreased to normal level in Gel-FA group. DNA fragmentations can be observed in apoptotic cells [40]. The results of TUNEL staining also showed that there were lots of TUNEL-positive cells in the Gel group (Fig. 4. 12(b)). Whereas, there was significantly

less TUNEL-positive cells in Gel-FA group (Fig. 4. 12(c)). Li et al. [75] suggested that resveratrol, an antioxidant, can down-regulate the expression of IL-1 which might response to oxidative stress induced apoptosis. Kim et al. [36] reported that caspase inhibitors can significantly inhibit the apoptosis of disc cells which induced by oxidative stress. In our study, the results demonstrated that FA can inhibit apoptosis in NP cells by inactivation of capase-3 activity.

5.3 The effects of thermosensitive ferulic acid-immobilized chitosan/gelatin/β-glycerol phosphate hydrogel on nucleus pulposus cells under hydrogen peroxide-induced oxidative stress

FA was immobilized on gelatin by EDC/NHS crosslinking method. The carboxyl group of FA can react to amino group of gelatin to form the amide bond. After immobilization, the residual amino group of gelatin was significantly decreased compared with gelatin group (without immobilization of FA) as shown in Fig. 4. 13. The results indicated that FA was successfully immobilized on C/G/GP hydrogel. The mechanism of antioxidant action of FA is through the hydroxyl group of FA which has the ability to donate a proton, and then to form the phenoxy radical. Phenoxy radical is a stable structure, which has five different resonance structures due to electron delocalization [44]. In this study, FA was immobilized on gelatin through amide bond formation; therefore, we believe that this immobilization process would not affect the antioxidant property of FA.

In the previous study [59], we suggested that the gelation mechanism of the thermosensitive C/G/GP hydrogel included hydrophobic interaction, hydrogen bonding, electrostatic interaction and molecular chain movement. The hydrophobic interactions have been assumed to be the main driving force to form the hydrogel consisting of

chitosan and gelatin at 37°C. This type of gelation mechanism has also been reported in other cases [54, 58]. In the study, we believe that the immobilization reaction between the carboxyl group of FA and the amino group of gelatin would not affect the gelation properties of developed hydrogel. The results of rheological analysis indicated that FA-immobilized C/G/GP solution could turn into a gel within 1 minute at 37°C and remain liquid for 15 minutes at 25°C (Fig. 4. 14). The results suggested that developed hydrogel also had good gelation and handling property for clinical application.

The results of cytotoxicity test showed that FA-immobilized C/G/GP hydrogel was biocompatible (Fig. 4. 15). The concentration of FA in the FA-immobilized C/G/GP hydrogel was 500 μM. In the study, we demonstrated that there was no significant cytotoxicity to NP cells if the concentration of FA was lower than 500 μM. Recent studies indicated that the apoptosis of NP cells could be induced by 100 μM H_2O_2 and the content of H_2O_2 was 0.13 ± 0.09 μmole in the human degenerative NP [34, 41]. As shown in Fig. 4. 2, we found that the oxidative stress induced by 100 μM H_2O_2 can be significantly decreased to normal level by 0.5 μM of FA. As shown in Fig. 4. 16(b), the cumulative concentration of FA released from developed hydrogel was 1.167 ± 0.179 μM within 30 minutes that was enough to stop the free radical reaction induced by 100 μM H_2O_2. As shown in Fig 4.8, the percentage of cumulative release of FA from

FA-incorporated C/G/GP hydrogel was 16.6 ± 2.1% in the first 2 hours, and it could be significantly decreased to 9.3 ± 0.7% in the FA-immobilized hydrogel (Fig. 4. 16(b)). The results demonstrated that immobilization of FA on C/G/GP hydrogel could sustain the delivery and prolong the release period of FA compared with the direct incorporation of FA.

Oxidative stress can induce inflammation through activation of nuclear factor-kappa B (NF-κB) and then up-regulate the expression of pro-inflammatory gene such as *IL-1β* and *iNOS* [45-76]. As shown in Fig. 4. 17, the mRNA gene expression of *iNOS* and *IL-1β* were significantly up-regulated in C/G/GP group compared with control group. Anti-inflammatory effects of FA have been demonstrated in recent years [44, 77]. FA is a phenolic acid which can inhibit the activation of NF-κB by inhibition of IκB kinase activity and down-regulate the expression of pro-inflammatory genes [45]. Fig. 4. 17 showed that there was no significant difference in the expression of *iNOS* and *IL-1β* between the FA-immobilized C/G/GP group and control group. The results indicated that FA release from the developed hydrogel could reduce the level of inflammation caused by oxidative stress.

In the degenerative NP, the imbalance between anabolisms and catabolism of the ECM results in loss of proteoglycans, decrease in type II collagen and increase in type I

collagen [1, 8, 18]. As shown in Fig. 4. 17, the expression of *type II collagen* and *aggrecan* were significantly down-regulated in C/G/GP group compared with control group. There was no significant difference in the expression of *aggrecan* between the control group and FA-immobilized C/G/GP group. The expression of *type II collagen* was significantly up-regulated in FA-immobilized C/G/GP group compared with other groups. Recent studies showed that polyphenol has the ability to prevent proteoglycan degradation [75]. In the study, we believe that FA might not only prevent proteoglycan degradation but also promote type II collagen synthesis. Urban et al. [1] indicated that the changes of proteoglycan are more obvious than those of collagen in the degenerative NP. As shown in Fig. 4. 17, there was no significant difference in the expression of *type I collagen* between the control group and experimental group (C/G/GP and FA-immobilized C/G/GP group).

In the normal NP, there is a balance between MMPs and TIMPs. MMPs have ability to degrade ECM components including proteoglycans and type II collagen [2]. Recent studies indicated that overproduction of ROS can promote MMPs production through an increase of pro-inflammatory mediators [4, 45]. Activation of MMPs can induce the expression of TGF-β which can inhibit the MMPs activity by up-regulation of TIMPs [4, 78]. As shown in Fig. 4. 17, the expression of *MMP-3*, *TIMP-1* and *TGF-β*

were significantly up-regulated in C/G/GP group compared with control group. The results suggested that the up-regulation of *TGF-β* might reflect that H_2O_2-induced oxidative stress NP cells attempt to balance the rate of synthesis and degradation of matrix by up-regulation of *TIMP-1*. There was no significant difference in the expression of *MMP-3*, *TIMP-1* and *TGF-β* between the FA-immobilized C/G/GP group and control group. High expression of TGF-*β* has been observed in the degenerative NP that is associated with inflammation [9, 22]. The results showed that FA could reduce cellular inflammation caused by oxidative stress. BMP-7 and IGF-1 are known as anabolic factors which can stimulate the proteoglycans and collagen synthesis [21]. As shown in Fig. 4. 17, there was no significant difference in the expression of *BMP-7* and *IGF-1* between the experimental group and the control group.

Aggrecan is a major proteoglycan in the NP and consists of core protein with attached glycosaminoglycan (GAG) including chondroitin sulfate and keratin sulfate. The decrease in the GAG content has been observed in the degenerative NP [1]. Fig. 4. 18 showed that the sulfated GAG production per cell was significantly decreased in C/G/GP group compared with other groups. The sulfated GAG content was reached to the normal level in the FA-immobilized C/G/GP group.

Oxidative stress mediated apoptosis occurs *via* intrinsic pathway which promotes

the release of cytochrome c from mitochondria and activates the caspase-9 activity. Activation of caspase-9 can lead to activation of caspase-3 which can cleave cellular substrate and result in apoptosis [37-39]. As shown in Fig. 4. 19, the caspase-3 activity was significantly increased in C/G/GP group compared with control group. The caspase-3 activity was decreased to normal level in FA-immobilized C/G/GP group. The results of TUNEL staining showed that there were lots of TUNEL-positive cells in C/G/GP group (Fig. 4. 20(b)), but only a few TUNEL-positive cells in both control group (Fig. 4. 20(a)) and FA-immobilized C/G/GP group (Fig. 4. 20(c)). Recent studies indicated that high level of ROS can directly damage both cells and ECM [71-73]. Polyphenol family has been demonstrated to have ability to inhibit apoptosis by decreasing ROS levels [45, 75]. FA processes an excellent antioxidant property that can inhibit oxidant reaction caused by ROS. In the study, the results showed that FA could inhibit the apoptosis of H_2O_2-induced oxidative stress NP cells and prevent further cellular damage.

CHAPTER 6 CONCLUSSION

The study demonstrated that 500 μM of FA might be the threshold dose to treat NP cells without cytotoxicity. From the results of mRNA gene expression, post-treatment of FA on H_2O_2-induced oxidative stress NP cells could restore part of the cell functions (*Aggrecan* and *MMP-3*) and promote the desired gene expression (*type II collagen* and *BMP-7*). The results of sulfated GAGs to DNA ratio and alcian blue stain indicated that the GAGs production could be switched back to the normal level in H_2O_2-induced oxidative stress NP cells. The results of caspase-3 activity and TUNEL stain revealed that the addition of FA to H_2O_2-induced oxidative stress NP cells decreased the apoptosis.

The study demonstrated that 500 μM of FA-incorporated C/G/GP hydrogel could significantly decrease the oxidative stress induced by 100 μM H_2O_2. From results of mRNA gene expression, FA-incorporated C/G/GP hydrogel could treat H_2O_2-induced oxidative stress NP cells through down-regulation of *MMP-3* and up-regulation *Aggrecan*; moreover, FA-incorporated C/G/GP hydrogel could promote the desired ECM-related gene expression (*type II collagen*). The results of sulfated GAGs to DNA ratio and alcian blue staining showed that the GAGs production of 100 μM

H_2O_2-induced oxidative stress NP cells could be increased to the normal level. The results of caspase-3 activity and TUNEL staining indicated that FA-incorporated C/G/GP hydrogel decreased the apoptosis of 100 μM H_2O_2-induced oxidative stress NP cells.

FA-immobilized C/G/GP hydrogel is liquid form at room temperature and turn into a gel at body temperature. FA-immobilized C/G/GP hydrogel is biocompatible. The immobilization of FA on C/G/GP hydrogel could prolong the release period of FA. From the results of mRNA gene expression, FA-immobilized C/G/GP hydrogel might treat H_2O_2-induced oxidative stress NP cells through down-regulation of *MMP-3* and up-regulation *Aggrecan* and *type II collagen*. The sulfated GAG production of 100 μM H_2O_2-induced oxidative stress NP cells could be increased to the normal level in the post-treatment of FA-immobilized C/G/GP hydrogel group. The results of caspase-3 activity and TUNEL staining show that the apoptosis of NP cells caused by oxidative stress could be inhibited by post-treatment of FA-immobilized C/G/GP hydrogel.

From the results of the study, FA could be used as a therapeutic molecule for NP regeneration and FA-incorporated C/G/GP hydrogel might be potentially applied as a long-term release system. The immobilization of FA on C/G/GP hydrogel could significantly prolong the release period of FA compared with direct incorporation of FA.

These results suggest that combination of FA and thermosensitive C/G/GP hydrogel may have potential application for NP regeneration in the near future.

References

[1] Urban JP, Roberts S. Degeneration of the intervertebral disc. Arthritis Research & Therapy 2003; 5:120-30.

[2] Goupille P, Jayson MI, Valat JP, Freemont AJ. Matrix metalloproteinases: The clue to intervertebral disc degeneration? Spine 1998; 23(14):1612-26.

[3] Roughley PJ. Biology of intervertebral disc aging and degeneration. Spine 2004; 29(23):2691-9

[4] Hadjipavlou AG, Tzermiadianos MN, Bogduk N, Zindrick MR. The pathophysiology of disc degeneration: a critical review. J Bone Joint Surg Br. 2008; 90:1261-70.

[5] Nerlich AG, Schleicher ED, Boos N. Immunohistologic markers for age-related changes of human lumbar intervertebral discs. Spine 1997; 22:2781-95.

[6] Urban JP, Smith S, Fairbank JC. Nutrition of the intervertebral disc. Spine 2004; 29(23):2700-9.

[7] Roberts S, Caterson B, Menage J, Evans EH, Jaffray DC, Eisenstein SM. Matrix metalloproteinases and aggrecanase: their role in disorders of the human intervertebral disc. Spine 2000; 25:3005-13.

[8] Anderson DG, Tannoury C. Molecular pathogenic factors in symptomatic disc degeneration. Spine J. 2005; 5:260-66.

[9] Peng B, Hao J, Hou S, Wu W, Jiang D, Fu X, Yang Y. Possible pathogenesis of painful intervertebral disc degeneration. Spine 2006; 31:560-6.

[10] An H, Boden SD, Kang J, Sandhu HS, Abdu W, Weinstein J. Summary statement: *emerging technique for treatment of degenerative lumbar disc disease.* Spine 2003; 28:24-5.

[11] Lee CK. Accelerated degeneration of the segment adjacent to a lumbar fusion. Spine 1988; 13:375-7.

[12] Yoon ST. Molecular therapy of the intervertebral disc. Spine J. 2005; 5:280-6.

[13] Paesold G, Nerlich AG, Boos N. Biological treatment strategies for disc degeneration: potentials and shortcomings. Eur Spine J. 2007; 16:447-68.

[14] Zhang Y, An HS, Tannoury C, Thonar EJ, Freedman MK, Anderson DG. Biological treatment for degenerative disc disease: implications for the field of physical medicine and rehabilitation. Am J Phys Med Rehabil 2008; 87:694-702.

[15] Alini M, Roughley PJ, Antoniou J, Stoll T, Aebi M. A biological approach to treating disc degeneration: not for today, but maybe for tomorrow. Eur Spine J.

2002; 11:S215-20.

[16] Cassinelli EH, Hall RA, Kang JD. Biochemistry of intervertebral disc degeneration and the potential for gene therapy applications. Spine J 2001; 1:205-14.

[17] Thompson JP, Pearce RH, Schechter MT, Adams ME, Tsang IK, Bishop PB. Preliminary evaluation of a scheme for grading the gross morphology of the human intervertebral disc. Spine 1990; 15:411-5.

[18] Roughley PJ. Biology of intervertebral disc aging and degeneration: involvement of the extracellular matrix. Spine 2004; 29:2691-9.

[19] Kanemoto M, Hukuda S, Komiya Y, Katsuura A, Nishioka J. Immunohistochemical study of matrix metalloproteinase-3 and tissue inhibitor of metalloproteinase-1 human intervertebral discs. Spine 1996; 21:1-8.

[20] Kang JD, Stefanovic-Racic M, McIntyre LA, Georgescu HI, Evans CH. Toward a biochemical understanding of human intervertebral disc degeneration and herniation. Contributions of nitric oxide, interleukins, prostaglandin E2, and matrix metalloproteinases. Spine (Phila Pa 1976). 1997; 22:1065-73.

[21] Masuda K, Oegema TR Jr, An HS. Growth factors and treatment of intervertebral disc degeneration. Spine 2004; 29:2757-69.

[22] Sowa G, Vadalà G, Studer R, Kompel J, Iucu C, Georgescu H, et al. Characterization of intervertebral disc aging. Spine 2008; 33:1821-8.

[23] Sobajima S, Shimer AL, Chadderdon RC, Kompel JF, Kim JS, Gilbertson LG et al. Quantitative analysis of gene expression in a rabbit model of intervertebral disc degeneration by real-time polymerase chain reaction. Spine J. 2005; 5:14-23.

[24] Tertti M, Paajanen H, Laato M, Aho H, Komu M, Kormano M. Disc degeneration in magnetic resonance imaging. A comparative biochemical, histologic, and radiologic study in cadaver spines. Spine 1991; 16:629-34.

[25] Zhao W, Zhao T, Chen Y, Ahokas RA, Sun Y. Zhao W, Zhao T, Chen Y, Ahokas RA, Sun Y. Oxidative stress mediates cardiac fibrosis by enhancing transforming growth factor-beta1 in hypertensive rats. Mol Cell Biochem. 2008; 317:43-50.

[26] Sullivan DE, Ferris M, Pociask D, Brody AR. The latent form of TGFbeta(1) is induced by TNFalpha through an ERK specific pathway and is activated by asbestos-derived reactive oxygen species in vitro and in vivo. J Immunotoxicol. 2008; 5:145-9.

[27] Bellocq A, Azoulay E, Marullo S, Flahault A, Fouqueray B, Philippe C, Cadranel J, Baud L. Reactive oxygen and nitrogen intermediates increase transforming growth

factor-beta1 release from human epithelial alveolar cells through two different mechanisms. Am J Respir Cell Mol Biol. 1999; 21:128-36.

[28] Liu RM, Gaston Pravia KA. Oxidative stress and glutathione in TGF-β-mediated fibrogenesis. Free Radic Biol Med. 2010; 48:1-15.

[29] Allen RG, Tresini M. Oxidative stress and gene regulation. Free Radic Biol Med. 2000; 28:463-99.

[30] Valko M, Leibfritz D, Moncol J, Cronin MT, Mazur M, Telser J. Free radicals and antioxidants in normal physiological functions and human disease. Int J Biochem Cell Biol. 2007; 39:44-84.

[31] Finkel T, Holbrook NJ. Oxidants, oxidative stress and the biology of ageing. Nature. 2000; 408:239-47.

[32] Ben-Porath I, Weinberg RA. The signals and pathways activating cellular senescence. Int J Biochem Cell Biol. 2005; 37:961-76.

[33] Zhao CQ, Wang LM, Jiang LS, Dai LY. The cell biology of intervertebral disc aging and degeneration. Ageing Res Rev. 2007; 6:247-61.

[34] Kim KW, Chung HN, Ha KY, Lee JS, Kim YY. Senescence mechanisms of nucleus pulposus chondrocytes in human intervertebral discs. Spine J. 2009; 9:658-66.

[35] Gruber HE, Ingram JA, Norton HJ, Hanley EN Jr. Senescence in cells of the aging and degenerating intervertebral disc: immunolocalization of senescence-associated beta-galactosidase in human and sand rat discs. Spine 2007; 32:321-7.

[36] Kim KW, Ha KY, Lee JS, Rhyu KW, An HS, Woo YK. The apoptotic effects of oxidative stress and antiapoptotic effects of caspase inhibitors on rat notochordal cells. Spine 2007; 32: 2443-48.

[37] Earnshaw WC, Martins LM, Kaufmann SH. Mammalian caspases: structure, activation, substrates, and functions during apoptosis. Annu Rev Biochem. 1999; 68:383-424.

[38] Nuñez G, Benedict MA, Hu Y, Inohara N. Caspases: the proteases of the apoptotic pathway. Oncogene 1998; 17:3237-45.

[39] Budihardjo I, Oliver H, Lutter M, Luo X, Wang X. Biochemical pathways of caspase activation during apoptosis. Annu Rev Cell Dev Biol. 1999; 15:269-90.

[40] Higuchi Y. Chromosomal DNA fragmentation in apoptosis and necrosis induced by oxidative stress. Biochem Pharmacol. 2003; 66:1527-35.

[41] Wei A, Brisby H, Chung SA, Diwan AD. Bone morphogenetic protein-7 protects human intervertebral disc cells in vitro from apoptosis. The spine journal 2008; 8:

466-474.

[42] Pandey KB, Rizvi SI. Plant polyphenols as dietary antioxidants in human health and disease. Oxid Med Cell Longev. 2009; 2:270-8.

[43] Kikuzaki H, Hisamoto M, Hirose K, Akiyama K, Taniguchi H. Antioxidant properties of ferulic acid and its related compounds. J Agric Food Chem. 2002; 50:2161-8.

[44] Srinivasan M, Sudheer AR, Menon VP. Ferulic Acid therapeutic potential through its antioxidant property. J Clin Biochem Nutr. 2007; 40:92-100.

[45] Rahman I, Biswas SK, Kirkham PA. Regulation of inflammation and redox signaling by dietary polyphenols. Biochem Pharmacol. 2006; 72:1439-52

[46] Kanski J, Aksenova M, Stoyanova A, Butterfield DA. Ferulic acid antioxidant protection against hydroxyl and peroxyl radical oxidation in synaptosomal and neuronal cell culture systems in vitro structure-activity studies. J Nutr Biochem. 2002; 13:273-281.

[47] Sudheer AR, Muthukumaran S, Kalpana C, Srinivasan M, Menon VP. Protective effect of ferulic acid on nicotine-induced DNA damage and cellular changes in cultured rat peripheral blood lymphocytes: a comparison with N-acetylcysteine.

Toxicol In Vitro. 2007; 21:576-85.

[48] Prasad NR, Ramachandran S, Pugalendi KV, Menon VP. Ferulic acid inhibits UV-B–induced oxidative stress in human lymphocytes. Nutrition Research 2007; 27:559-64.

[49] Srinivasan M, Sudheer AR, Pillai KR, Kumar PR, Sudhakaran PR, Menon VP. Influence of ferulic acid on γ-radiation induced DNA damage, lipid peroxidation and antioxidant status in primary culture of isolated rat hepatocytes. Toxicology. 2006; 228:249-58.

[50] Balasubashini MS, Rukkumani R, Viswanathan P, Menon VP. Ferulic acid alleviates lipid peroxidation in diabetic rats. Phytother Res. 2004; 18:310-4.

[51] Drury JL, Mooney DJ. Mooney. Hydrogels for tissue engineering: scaffold design variables and applications. Biomaterials 2003; 24:4337-51.

[52] Ruel-Gariépy E, Leroux JC. In situ-formation hydrogels--review of temperature-sensitive systems. Eur J Pharm Biopharm. 2004; 58:409-26.

[53] Ta HT, Dass CR, Dunstan DE. Injectable chitosan hydrogels for localised cancer therapy. J Control Release 2008; 126:205-16.

[54] Bhattarai N, Ramay HR, Gunn J, Matsen FA, Zhang M. PEG-grafted chitosan as an

injectable thermosensitive hydrogel for sustained protein release. J Control Release. 2005; 103:609-24.

[55] Chenite A, Chaput C, Wang D, Combes C, Buschmann MD, Hoemann CD, et al. Novel injectable neutral solutions of chitosan form biodegradable gels in situ. Biomaterial 2000; 21:2155-61.

[56] Chenite A, Buschmann M, Wang D, Chaput C, Kandani N. Reheological characterisation of thermogelling chitosan/glycerol-phospate solution. Carbohydrate Polymers 2001; 46:39-47.

[57] Berger J, Reist M, Chenite A, Felt-Baeyens O, Mayer JM, Gurny R. Pseudo-thermosetting chitosan hydrogels for biomedical application. International Journal of Pharmaceutics 2005; 288:197-206.

[58] Roughley P, Hoemann C, DesRosiers E, Mwale F, Antoniou J, Alini M. The potential of chitosan-based gels containing intervertebral disc cells for nucleus pulposus supplementation. Biomaterials 2006; 27:388-96.

[59] Cheng YH, Yang SH, Su WY, Chen YC, Yang KC, Lin FH et al. Thermosensitive chitosan-gelatin-glycerol phosphate hydrogels as a cell carrier for nucleus pulposus regeneration: an in-vitro study. Tissue Eng Part A. 2010; 16:695-703.

[60] Tang YF, Du YM, Hu XW, Shi XW, Kennedy JF. Rheological characterisation of a novel thermosensitive chitosan/poly(vinyl alcohol) blend hydrogel. Carbohydrate Polymers 2007; 67:491-9.

[61] Bhattarai N, Gunn J, Zhang M. Chitosan-based hydrogels for controlled, localized drug delivery. Adv Drug Deliv Rev. 2010; 62:83-99.

[62] Ruel-Gariépy E, Chenite A, Chaput C, Guirguis S, Leroux J. Characterization of thermosensitive chitosan gels for the sustained delivery of drugs. Int J Pharm. 2000; 203:89-98.

[63] Ruel-Gariépy E, Shive M, Bichara A, Berrada M, Le Garrec D, Chenite A, et al. A thermosensitive chitosan-based hydrogel for the local delivery of paclitaxel. Eur J Pharm Biopharm. 2004; 57:53-63.

[64] Wu J, Su ZG, Ma GH. A thermo- and pH-sensitive hydrogel composed of quaternized chitosan/glycerophosphate. Int J Pharm. 2006; 315:1-11.

[65] Komeima K, Rogers BS, Lu L, Campochiaro PA. Antioxidants reduce cone cell death in a model of retinitis pigmentosa. Proc Natl Acad Sci U S A. 2006; 103:11300-5.

[66] Fiorito C, Rienzo M, Crimi E, Rossiello R, Balestrieri ML, Casamassimi A et al.

Antioxidants increase number of progenitor endothelial cells through multiple gene expression pathways. Free Radical Research 2008; 42:754-62.

[67] Rao GN, Corson MA, Berk BC. Uric acid stimulates vascular smooth muscle cell proliferation by increasing platelet-derived growth factor A-chain expression. J Biol Chem. 1991; 266:8604-8.

[68] Blokhina O, Virolainen E, Fagerstedt KV. Antioxidants, oxidative damage and oxygen deprivation stress: a review. Ann Bot. 2003; 91:179-94.

[69] Masuda K, An HS. Growth factors and the intervertebral disc. The Spine Journal 2004; 4:330-40.

[70] Lipson SJ, Muir H. Vertebral osteophyte formation in experimental disc degeneration. Morphologic and proteoglycan changes over time. Arthritis Rheum. 1980; 23:319-24.

[71] Stern R, Kogan G, Jedrzejas MJ, Soltés L. The many ways to cleave hyaluronan. Biotechnol Adv. 2007; 25:537-57.

[72] Walker MH, Anderson DG. Molecular basis of intervertebral disc degeneration. Spine J. 2004; 4:158-66.

[73] Rodriguez E, Roughley P. Link protein can retard the degradation of hyaluronan in

proteoglycan aggregates. Osteoarthritis Cartilage 2006; 14:823-9.

[74] Hengartner MO. The biochemistry of apoptosis. Nature 2000; 407:770-6.

[75] Li X, Phillips FM, An HS, Ellman M, Thonar EJ, Wu W et al. The Action of Resveratrol, a phytoestrogen found in grapes, on the intervertebral disc. Spine 2008; 33:2586-95.

[76] Martindale JL, Holbrook NJ. Cellular response to oxidative stress: signaling for suicide and survival. J Cell Physiol. 2002; 192:1-15.

[77] Barone E, Calabrese V, Mancuso C. Ferulic acid and its therapeutic potential as a hormetin for age-related diseases. Biogerontology 2009; 10:97-108.

[78] Grimm T, Schäfer A, Högger P. Antioxidant activity and inhibition of matrix metalloproteinases by metabolites of maritime pine bark extract (pycnogenol). Free Radic Biol Med. 2004; 36:811-22.

Curriculum Vitae

Yung-Hsin Cheng
Institute of Biomedical Engineering
College of Medicine and College of Engineering
National Taiwan University
No.1, Jen Ai Road, Section 1, Taipei, 10051, Taiwan, R.O.C.
Tel: 886-972229725
E-mail: d97548005@ntu.edu.tw

Research Interests:
Biomaterials, Tissue engineering

Education:
Ph.D., Biomedical Engineering, National Taiwan University, Taiwan (2008/09-2012/06)
M.S., Biomedical Engineering, National Taiwan University, Taiwan (2006/09-2008/06)
BEng., Polymer Engineering, National Taiwan University of Science and Technology, Taiwan (2002/09-2006/06)

Publications:
1. Cheng YH, Yang SH, Lin FH. Thermosensitive chitosan-gelatin-glycerol phosphate hydrogel as a controlled release system of ferulic acid for nucleus pulposus regeneration. Biomaterials 2011; 32:6953-61. (SCI, IF:7.882, Rank: 2/69)
2. Cheng YH, Yang SH, Yang KC, Chen MP, Lin FH. The effects of ferulic acid on nucleus pulposus cells under hydrogen peroxide-induced oxidative stress. Process Biochem. 2011; 46:1670-7. (SCI, IF:2.648, Rank: 17/134)
3. Cheng YH, Yang SH, Su WY, Chen YC, Yang KC, Cheng WT, Wu SC, Lin FH. Thermosensitive chitosan-gelatin-glycerol phosphate hydrogels as a cell carrier for nucleus pulposus regeneration: an in-vitro study. Tissue Eng Part A. 2010; 16:695-703. (SCI, IF: 4.636, Rank: 20/160)
4. Chen MP, Yang SH, Chou CH, Yang KC, Wu CC, Cheng YH, Lin FH. The chondroprotective effects of ferulic acid on hydrogen peroxide-stimulated chondrocytes: inhibition of hydrogen peroxide-induced pro-inflammatory cytokines and metalloproteinase gene expression at the mRNA level. Inflamm Res. 2010; 59:587-95. (SCI, IF: 2.004, Rank: 99/134)

5. Yang KC, Wu CC, Cheng YH, Kuo TF, Lin FH. Chitosan/gelatin hydrogel prolonged the function of insulinoma/agarose microspheres in vivo during xenogenic transplantation. Transplant Proc. 2008; 40:3623-6. (SCI, IF: 0.993, Rank: 117/188)
6. Yang KC, Wu CC, Lin FH, Qi Z, Kuo TF, Cheng YH, Chen MP, Sumi S. Chitosan/gelatin hydrogel as immunoisolative matrix for injectable bioartificial pancreas. Xenotransplantation 2008; 15:407-16. (SCI, IF: 2.067, Rank: 52/106)

Conference:

1. Tissue Engineering and Regenerative Medicine International Society (TERMIS EU 2011), Granada, Spain. Oral presentation, "The Effects of Ferulic Acid on Nucleus Pulposus Cells under Hydrogen Peroxide-induced Oxidative Stress".
2. International Symposium of Materials on Regenerative Medicine (2010 ISOMRM), Miaoli , Taiwan. Poster presentation, "The Effects of Ferulic Acid on Nucleus Pulposus Cells under Hydrogen Peroxide-induced Oxidative Stress"
3. 15th Biomedical Science and Technology Symposium (BIOMED 2009), Northern Cyprus Campus, Turkey. Poster presentation, "Thermosensitive Chitosan-Gelatin-Glycerol Phosphate Hydrogels as a Cell Carrier for Nucleus Pulposus Regeneration".
4. 2009 Annual Meeting of Formosa Association of Regenerative Medicine, Taipei, Taiwan. Oral presentation, "Thermosensitive Chitosan-Gelatin-Glycerol Phosphate Hydrogels as a Cell Carrier for Nucleus Pulposus Regeneration".

Awards:

1. Graduate Students Study Abroad Program. 2011 National Science Council. Nov 29, 2011
2. Excellent Research Award. 2009 Annual Meeting of Formosa Association of Regenerative Medicine, Taipei, Taiwan. Feb 14, 2009

International Connections:

1. Visiting Student, Department of Bioengineering, University of Washington, Seattle, USA. March, 2012
2. Visiting Student, Department of Biomedical Engineering, Tel Aviv University, Tel Aviv, Israel. August, 2011
3. Scientific Co-chair, Student and Young Investigator Section (SYIS) Activity, TEMIS EU 2011, Granada, Spain. June, 2011

Training Course:

1. Education and Traning in the Care and Use of Laboratory Animal. Laboratory Animal Center, National Taiwan University, Taipei, Taiwan. April, 2010
2. Atomic Force Microscopy Bioworkshop, National Health Research Institutes, Miaoli, Taiwan. July, 2009
3. Atomic Force Microscopy in Biology Class, Asylum Research, Santa Barbara, CA, USA. April, 2008

Teaching experience:

1. Teaching Assistant, Summer Course of Stem Cell and Tissue Engineering. Center of Biotechnology, National Taiwan University. August, 2011
2. Teaching Assistant, Summer Course of Stem Cell and Tissue Engineering. Center of Biotechnology, National Taiwan University. August, 2010
3. Teaching Assistant, Summer Course of Stem Cell and Tissue Engineering. Center of Biotechnology, National Taiwan University. August, 2009